

Accessing the Triplet Manifold of Naphthalenebenzimidazole-Phenanthroline in Rhenium(I) Bichromophores

Kaylee A. Wells,^{*a} James E. Yarnell,^{a,b} Sara Sheykhi,^a Jonathan R. Palmer,^a Daniel T. Yonemoto,^a Rosalynd Joyce,^a Sofia Garakyaraghı,^a and Felix N. Castellano^a

Table of Contents

Chemicals and Characterization Data	2
Additional Computational Data	20
Additional Spectroscopic Data.....	34

Chemicals and Characterization Data

All chemicals and solvents were analytical grade, and they were used without further purification. Nuclear magnetic resonance (NMR) spectra were measured at 298 K with a Bruker® Avance NEO 700 MHz (¹H) and 176 MHz (¹³C) and processed with MestreNova software (version 10.0.2), with the chemical shifts referenced to residual solvent signals. The chemical shifts (δ ppm) are referenced to the respective solvent and splitting patterns are designed as s (singlet), d (doublet), t (triplet), m (multiplet). High resolution electrospray ionization mass spectrometry (HR-ESI-MS) was measured by the Michigan State University Mass Spectrometry Core, East Lansing, MI. MS values are given as m/z.

Synthesis of 16H-benzo[4',5']isoquinolino[2',1':1,2]imidazo[4,5-f][1,10]phenanthrolin-16-one (**NBI-phen**). NBI-phen was synthesized with modification to the previously reported procedure.¹ 5,6-Diamino-1,10-phenanthroline (1.46 mmol, 308 mg) and 1,8-naphthalic anhydride (2.01 mmol, 398 mg) were mixed in 30 mL of acetic acid which was degassed with nitrogen. This mixture was then heated for 24 hours at 140 °C. After addition of water and a saturated, aqueous solution of sodium carbonate the ligand began to precipitate and was then filtered off on a glass frit and washed with water, ethanol, and diethyl ether. The resulting dark yellow solid was recrystallized in hot ethanol to give **NBI-phen** (64 %). ¹H NMR (700 MHz, CDCl₃) δ 10.80 (d, J = 8.7 Hz, 1H), 9.56 (d, J = 8.2 Hz, 1H), 9.36 (t, J = 5.3 Hz, 2H), 9.23 (d, J = 7.4 Hz, 1H), 9.17 (d, J = 7.4 Hz, 1H), 8.66 (d, J = 8.1 Hz, 1H), 8.59 (d, J = 8.2 Hz, 1H), 8.45 – 8.42 (m, 1H), 8.33 – 8.30 (m, 1H), 8.14 (dd, J = 11.4, 4.0 Hz, 1H), 8.11 (t, J = 7.8 Hz, 1H) ppm. ¹³C NMR (176 MHz, CDCl₃) δ 159.93, 151.64, 150.36, 144.93, 144.89, 139.16, 137.70, 137.44, 136.74, 135.76, 132.63, 132.25, 131.90, 129.08, 128.83, 128.02, 126.77, 126.29, 123.99, 121.76, 121.09, 120.94, 77.34, 77.16, 76.98, 21.26 ppm. MS [HR-ESI]: m/z calcd for C₂₄H₁₂N₄OH [M+H]⁺ 373.1089, found 373.1094.

Synthesis of Re(CO)₃(NBI-phen)Cl. Pentacarbonylchlororhenium(I) (1 mmol, 332 mg) was added to NBI-phen (1.1 mmol, 382 mg) and 80 mL of toluene in a 150 mL round bottom flask. The solution was degassed, put under N₂, and refluxed while mixing for 12 hours. After cooling, the yellow precipitate was filtered out on a glass frit and washed with 800 mL of toluene. The yellow solid was further purified using neutral alumina and eluted with dichloromethane and 10% acetonitrile to give Re(CO)₃(NBI-phen)Cl (89 %). ¹H-NMR (DMSO-d₆) δ 10.27 (d, J= 8.42 Hz, 1H), 9.53 (d, J= 4.45 Hz, 1H), 9.47 (d, J= 4.20 Hz, 1H), 9.39 (d, J= 6.96 Hz, 1H), 8.88 (d, J= 6.81 Hz, 1H), 8.84 (d, J= 6.65 Hz, 1H), 8.58 (d, J= 8.84 Hz, 1H), 8.41 (d, J= 8.25 Hz, 1H), 8.23 (m, 2H), 8.02-7.94 (m, 2H). MS [HR-ESI]: m/z calcd for [M-Cl]⁺ 643.04106, found 643.03910.

Synthesis of Re(CO)₃(NBI-phen)OTf. Re(CO)₃(NBI-phen)(Cl) (0.16 mmol, 109 mg) was added to 50 mL round bottom flask along with 20 mL of absolute ethanol. The solution was covered (dark), deaerated, put under N₂. Silver triflate (0.18 mmol, 47 mg) was added to the reaction mixture and refluxed for 6 hours. Once cool, the solution was filtered through celite on a glass frit to remove AgCl from solution. The yellow filtrate was dried under reduced pressure. The crude product was chromatographed using acidic alumina and eluted with acetonitrile to give Re(CO)₃(NBI-phen)OTf (80 %). MS [HR-ESI]: m/z calcd for [M-OTf]⁺ 643.04106, found 643.03964.

Synthesis of fac-[Re(NBI-phen)(CO)₃(PPh₃)](PF₆) (**Re1**). Re(CO)₃(NBI-phen)OTf (0.19 mmol, 150 mg) and PPh₃ (1.34 mmol, 350 mg) were added to 50mL round bottom flask along with 20mL acetonitrile. This mixture was then refluxed for 12 hours. The solvent was removed under reduced pressure and the crude product was chromatographed on acidic alumina with dichloromethane and increasing amounts of acetonitrile. The collected fraction was dissolved in minimal amount of methanol and precipitated as the PF₆ salt using a dropwise addition of an ammonium hexafluorophosphate solution in water (1.0 g in 10 mL). The solid was collected on a glass frit and washed with 250 mL of distilled water. The solid was recrystallized in dichloromethane and diethyl ether. The yellow solid was dried under vacuum overnight to give fac-[Re(NBI-phen)(CO)₃(PPh₃)](PF₆) (**Re1**) (96 %). ¹H NMR (700 MHz, DMSO) δ 10.16 (d, J = 8.6 Hz, 1H), 9.41 (d, J = 5.0 Hz, 1H), 9.31 (t, J = 7.0 Hz, 2H), 8.97 (d, J = 7.1 Hz, 1H), 8.93 (d, J = 7.2 Hz, 1H), 8.69 (d, J = 8.0 Hz, 1H), 8.53 (d, J = 8.1 Hz, 1H), 8.09 (t, J = 7.6 Hz, 1H), 8.07 – 8.00 (m, 3H), 7.35 (t, J = 7.4 Hz, 3H), 7.25 (t, J = 6.7 Hz, 6H), 7.01 – 6.97 (m, 6H) ppm. ¹³C NMR (176 MHz, DMSO) δ 194.95, 160.86, 155.04, 153.32, 152.42, 144.99, 144.44, 138.65, 138.32, 136.42, 134.14, 132.98, 132.86, 132.26, 132.20, 131.67, 131.05, 129.93, 129.13, 129.07, 128.08, 128.00, 127.82, 127.59, 127.50, 126.12, 125.99, 124.97, 124.47, 122.94, 122.59, 120.12, 40.02, 39.88, 39.76, 39.64, 39.52, 39.40, 39.28, 39.16 ppm. MS [HR-ESI]: m/z calcd for C₄₅H₂₇N₄O₄PRe [M]⁺ 903.1299, found 903.1307.

Synthesis of fac-[Re(NBI-phen)(CO)₃(CH₃CN)](PF₆) (**Re2**). Re(CO)₃(NBI-phen)Cl (0.10 mmol, 69 mg) and silver triflate (0.10 mmol, 26 mg) were suspended in 50 mL of freshly distilled acetonitrile. The solution was covered (dark), deaerated, put under N₂, and refluxed for 12 hours. Once cool, the reaction contents were filtered over celite to remove AgCl from solution. The filtrate was dried under reduced pressure and then dissolved in a minimal amount of methanol and precipitated as the PF₆ salt using a dropwise addition of an ammonium hexafluorophosphate solution in water (1.0 g in 10 mL). The solid was collected on a glass frit and washed with water and dried under vacuum to give fac-[Re(NBI-phen)(CO)₃(CH₃CN)](PF₆) (**Re2**) (71 %). ¹H NMR (700 MHz, CD₃CN) δ 10.48 (d, J = 8.6 Hz, 1H), 9.51 (t, J = 5.8 Hz, 2H), 9.47 (d, J = 4.8 Hz, 1H), 9.01 (d, J = 7.2 Hz, 1H), 8.96 (d, J = 7.2 Hz, 1H), 8.57 (d, J = 8.0 Hz, 1H), 8.42 (d, J = 8.1 Hz, 1H), 8.20 (ddd, J = 18.7, 8.4, 4.9 Hz, 2H), 8.01 (dt, J = 15.5, 7.7 Hz, 2H) ppm. ¹³C NMR (176 MHz, CD₃CN) δ 155.38, 153.88, 146.88, 140.41, 140.10, 137.58, 135.93, 134.30, 133.87, 132.96, 128.94, 128.82, 128.67, 128.11, 127.30, 127.00, 126.49, 126.28, 124.40, 123.87, 123.48, 121.29, 120.71, 118.26, 68.24, 26.20, 1.27, 1.15. MS [HR-ESI]: m/z calcd for C₂₉H₁₅N₅O₄Re [M]⁺ 682.0654, found 682.0661.

Synthesis of Re(CO)₃(phen)Cl. It was synthesized according to the previously reported procedure.² Pentacarbonylchlororhenium(I) (5.53 mmol, 2 g) was added to 1,10-phenanthroline (5.53 mmol, 1 g) and 30 mL of toluene in a 100 mL round bottom flask. The solution was degassed, put under N₂, and refluxed while mixing for 4 hours. After cooling, the yellow precipitate was filtered out on a glass frit and washed with 300 mL of toluene to give Re(CO)₃(phen)Cl (93 %). ¹H NMR (700 MHz, CD₂Cl₂) δ 9.42 – 9.36 (m, 1H), 8.62 (dd, J = 8.2, 0.8 Hz, 1H), 8.07 (s, 1H), 7.91 (dd, J = 8.2, 5.1 Hz, 1H). ¹³C NMR (176 MHz, CD₂Cl₂) δ 153.36, 147.35, 138.70, 131.28, 128.04, 126.25, 54.15, 53.99, 53.84, 53.68, 53.53. MS [HR-ESI]: m/z calcd for C₁₅H₈N₂O₃Re [M-Cl]⁺ 449.0064, found 449.0045.

Synthesis of Re(CO)₃(phen)OTf. Re(CO)₃(phen)(Cl) (3.1 mmol, 1.5 g) was added to 500 mL round bottom flask along with 300 mL of absolute ethanol. The solution was covered (dark), deaerated, put under N₂. Silver triflate (3.2 mmol, 0.82 g) was added to the reaction mixture and refluxed for 6 hours. Once cool,

the solution was filtered through celite on a glass frit to remove AgCl from solution. The yellow filtrate was dried under reduced pressure to give Re(CO)₃(phen)OTf (90 %). MS [HR-ESI]: m/z calcd for [M-OTf]⁺ 449.0064, found 449.0095.

Synthesis of fac-[Re(phen)(CO)₃(PPh₃)](PF₆) (**Mod1**). Re(CO)₃(phen)OTf (2.5 mmol, 1.5 g) and PPh₃ (25 mmol, 1 g) were added to 500mL round bottom flask along with 300mL tetrahydrofuran. This mixture was then refluxed for 12 hours. The solvent was removed to 90% under reduced pressure and product was precipitated as the PF₆ salt using a dropwise addition of an ammonium hexafluorophosphate solution in water (1.0 g in 10 mL). The solid was collected on a glass frit and washed with 250 mL of distilled water. The yellow solid was dried under vacuum overnight to give fac-[Re(phen)(CO)₃(PPh₃)](PF₆) (**Mod1**) (98 %). ¹H NMR (700 MHz, CD₃CN) δ 9.11 (dd, J = 5.1, 0.6 Hz, 2H), 8.62 (d, J = 8.2 Hz, 2H), 8.05 (s, 2H), 7.73 (dd, J = 8.2, 5.1 Hz, 2H), 7.33 (dt, J = 7.4, 3.7 Hz, 3H), 7.20 (td, J = 7.7, 2.1 Hz, 6H), 7.04 – 7.00 (m, 6H) ppm. ¹³C NMR (176 MHz, CD₃CN) δ 155.79, 147.18, 140.24, 133.51, 133.45, 131.95, 131.93, 129.94, 129.88, 129.65, 129.38, 128.87, 127.56, 118.26, 1.27 ppm. MS [HR-ESI]: m/z calcd for C₃₃H₂₃N₂O₃PRe [M]⁺ 711.0976, found 711.0970.

Synthesis of fac-[Re(phen)(CO)₃(CH₃CN)](PF₆) (**Mod2**). Re(CO)₃(phen)Cl (2.06 mmol, 1 g) were suspended in 300 mL of acetonitrile. The solution was covered (dark), deaerated, put under N₂. Silver triflate (2.12 mmol, 0.545 g) was added to the reaction mixture and refluxed for 12 hours. Once cool, the reaction contents were filtered over celite to remove AgCl from solution. The filtrate was dried under reduced pressure and then dissolved in a minimal amount of methanol and precipitated as the PF₆ salt using a dropwise addition of an ammonium hexafluorophosphate solution in water (1.0 g in 10 mL). The solid was collected on a glass frit and washed with water and dried under vacuum to give fac-[Re(phen)(CO)₃(CH₃CN)](PF₆) (**Mod2**) (91 %). ¹H NMR (400 MHz, CD₂Cl₂) δ 9.38 (dd, J = 5.1, 1.3 Hz, 2H), 8.80 (dd, J = 8.3, 1.3 Hz, 2H), 8.21 (s, 2H), 8.05 (dd, J = 8.3, 5.1 Hz, 2H), 2.06 (s, 3H), 1.54 (s, 3H) ppm. ¹³C NMR (176 MHz, CD₂Cl₂) δ 154.46, 147.24, 140.55, 131.72, 128.63, 127.13, 54.15, 54.00, 53.84, 53.69, 53.53, 3.70 ppm. MS [HR-ESI]: m/z calcd for C₁₇H₁₁N₃O₃Re [M]⁺ 490.0330, found 490.0339.

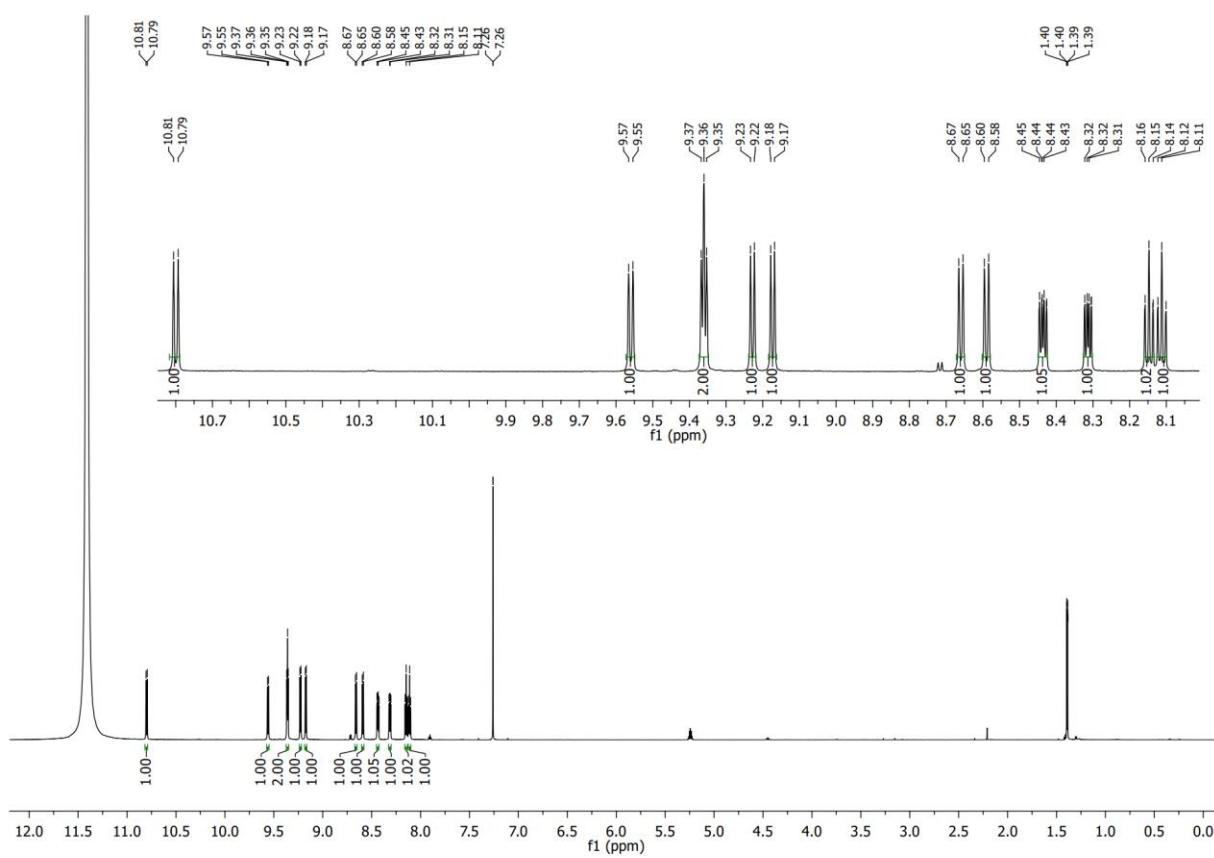


Figure S1. 700 MHz ^1H NMR of 16H-benzo[4',5']isoquinolino[2',1':1,2]imidazo[4,5-f][1,10]phenanthrolin-16-one (**NBI-phen**) in CDCl_3 at 300K.

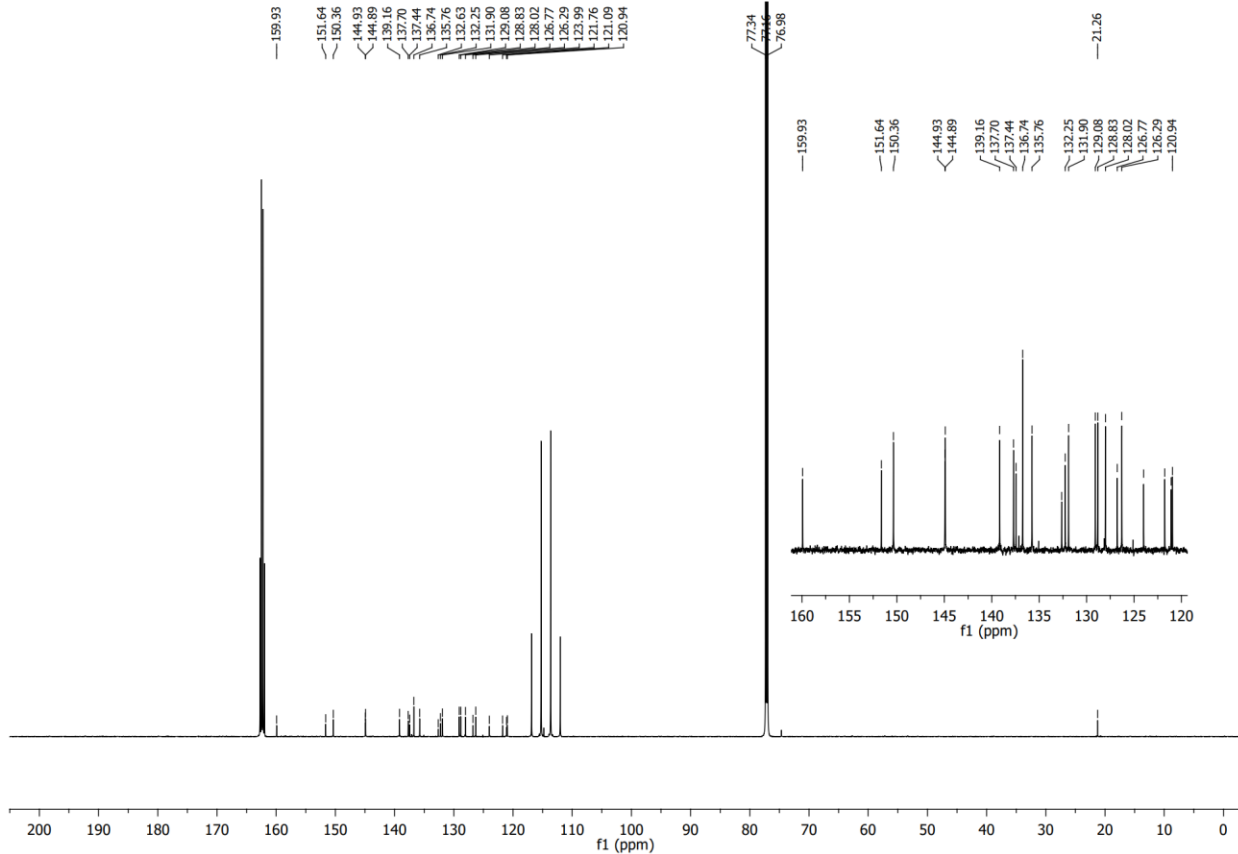


Figure S2. 176 MHz ^{13}C NMR of 16H-benzo[4',5']isoquinolino[2',1':1,2]imidazo[4,5-f][1,10]phenanthrolin-16-one (**NBI-phen**) in CDCl_3 at 300K.

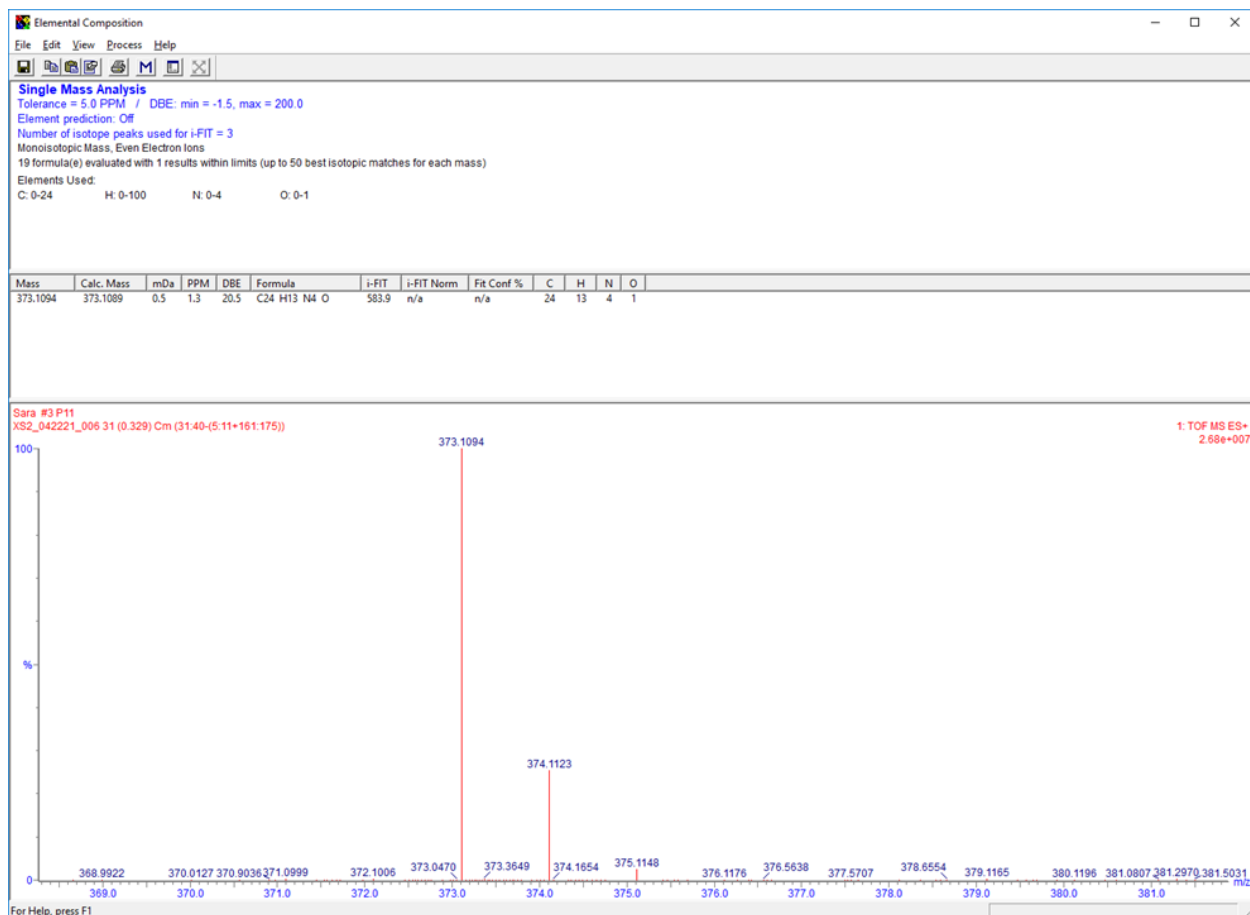


Figure S3. HR-ESIMS of 16H-benzo[4',5']isoquinolino[2',1':1,2]imidazo[4,5-f][1,10]phenanthrolin-16-one (NBI-phen).

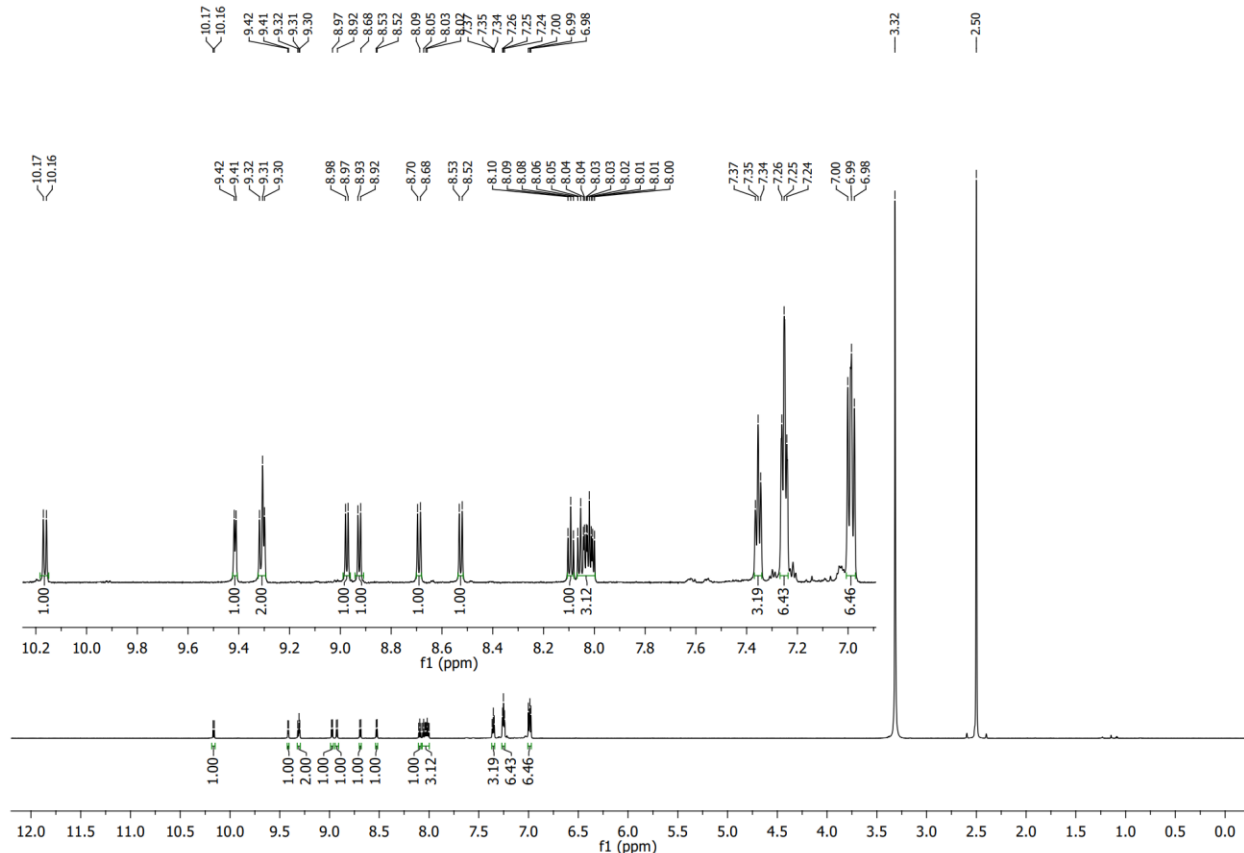


Figure S4. 700 MHz ^1H NMR of fac-[Re(NBI-phen)(CO)₃(PPh₃)](PF₆) (**Re1**) in DMSO at 300K.

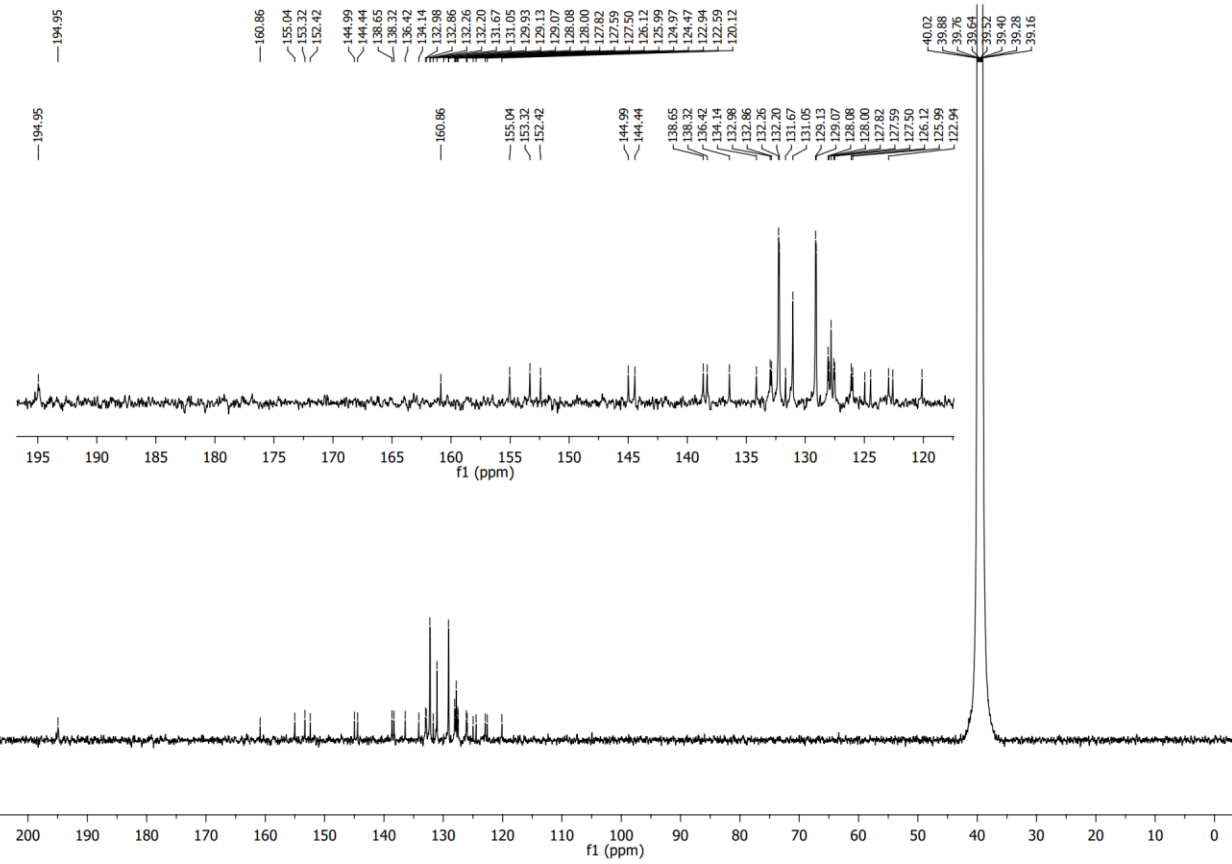


Figure S5. 176 MHz ^{13}C NMR of fac-[Re(NBI-phen)(CO)₃(PPh₃)](PF₆) (**Re1**) in DMSO at 300K.



Figure S6. HR-ESIMS of fac-[Re(NBI-phen)(CO)₃(PPh₃)](PF₆) (**Re1**).

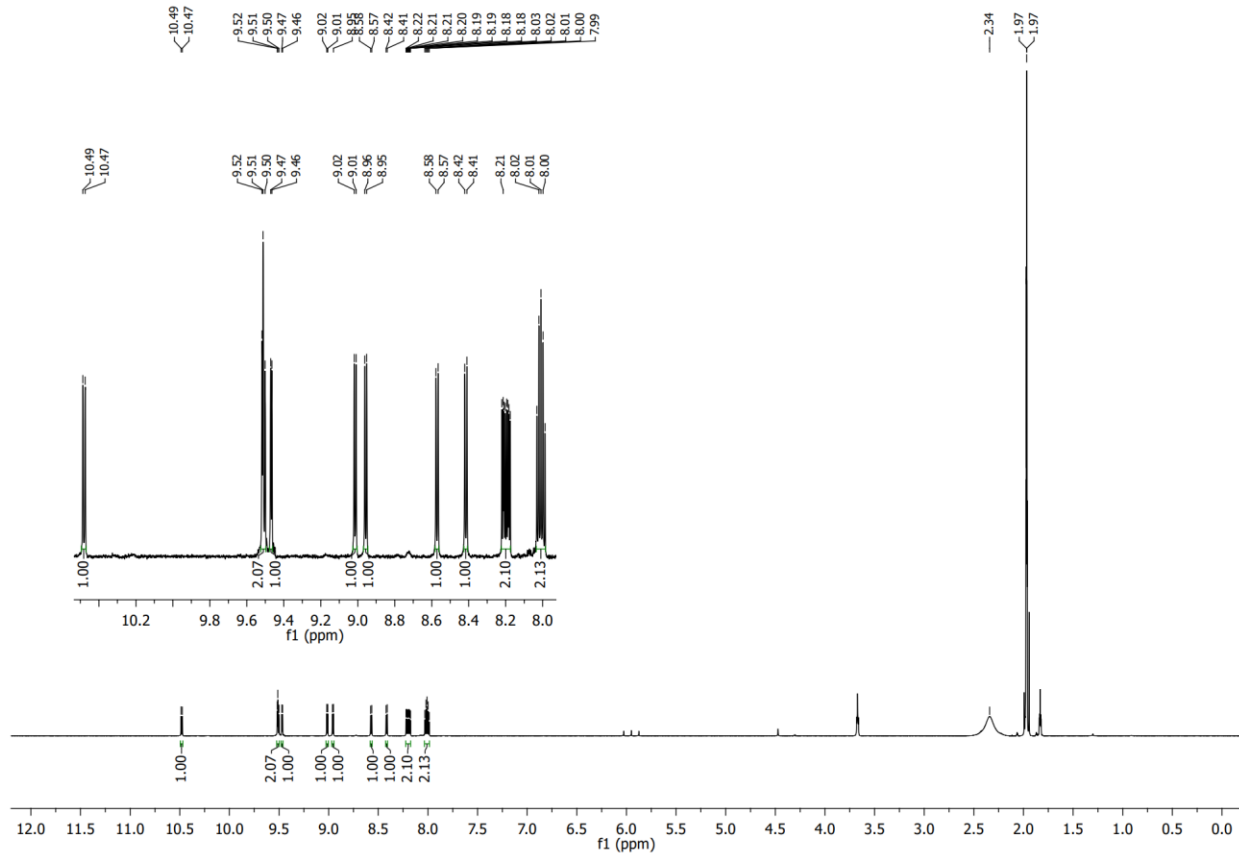


Figure S7. 700 MHz ¹H NMR of fac-[Re(NBI-phen)(CO)₃(CH₃CN)](PF₆) (**Re2**) in CD₃CN at 300K.

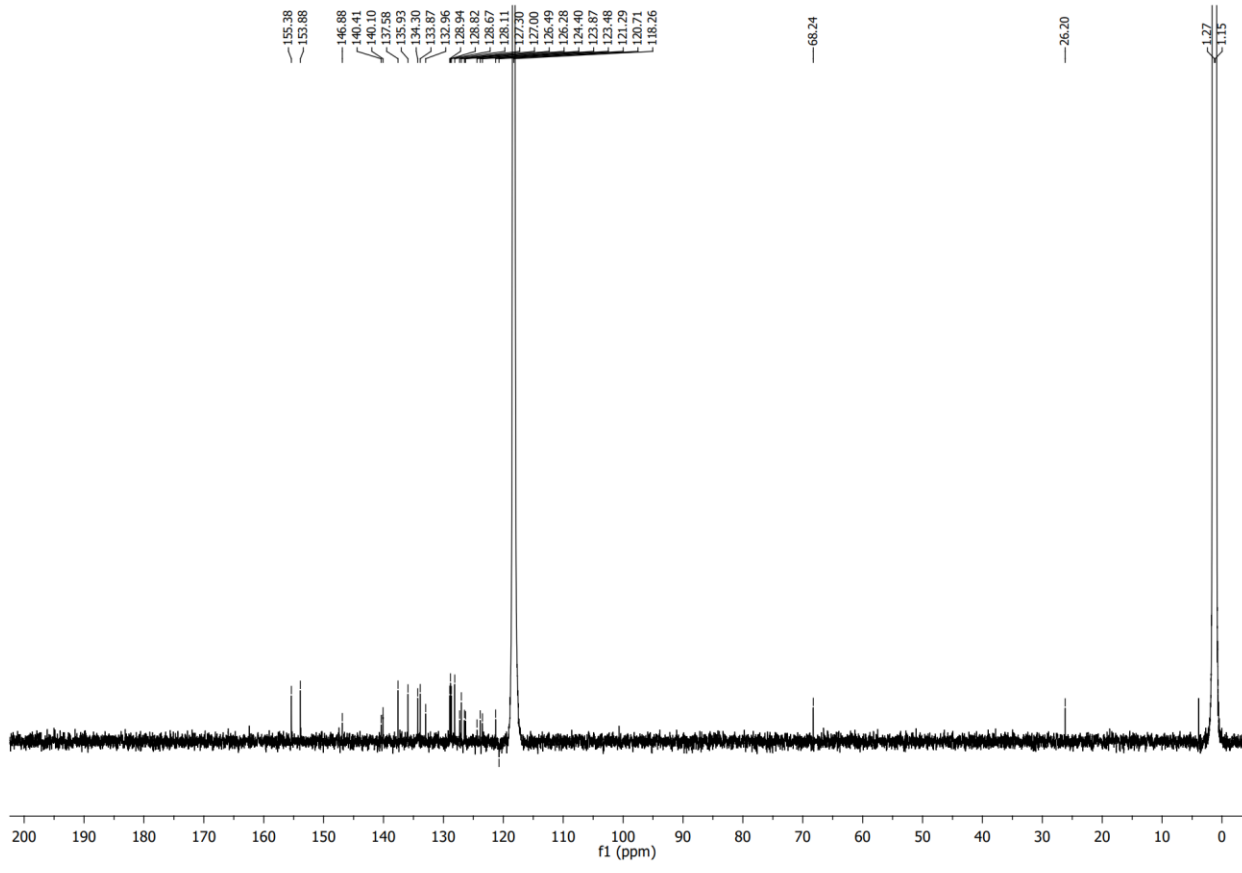


Figure S8. 176 MHz ^{13}C NMR of fac-[Re(NBI-phen)(CO) $_3$ (CH $_3$ CN)](PF $_6$) (**Re2**) in CH $_3$ CN at 300K.



Figure S9. HR-ESIMS of fac-[Re(NBI-phen)(CO)₃(CH₃CN)](PF₆) (**Re2**).

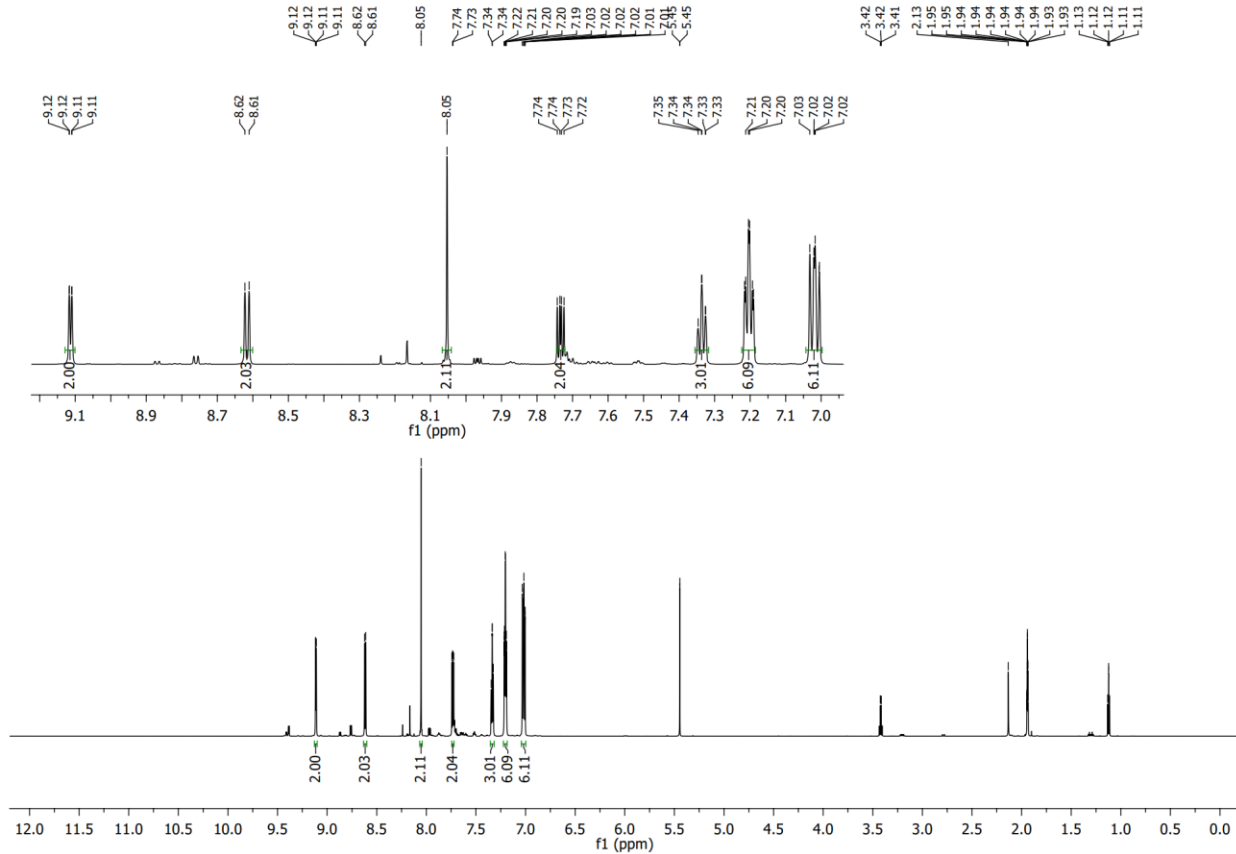


Figure S10. 700 MHz ^1H NMR of fac-[Re(phen)(CO)₃(PPh₃)](PF₆) (**Mod1**) in CD₃CN at 300K.

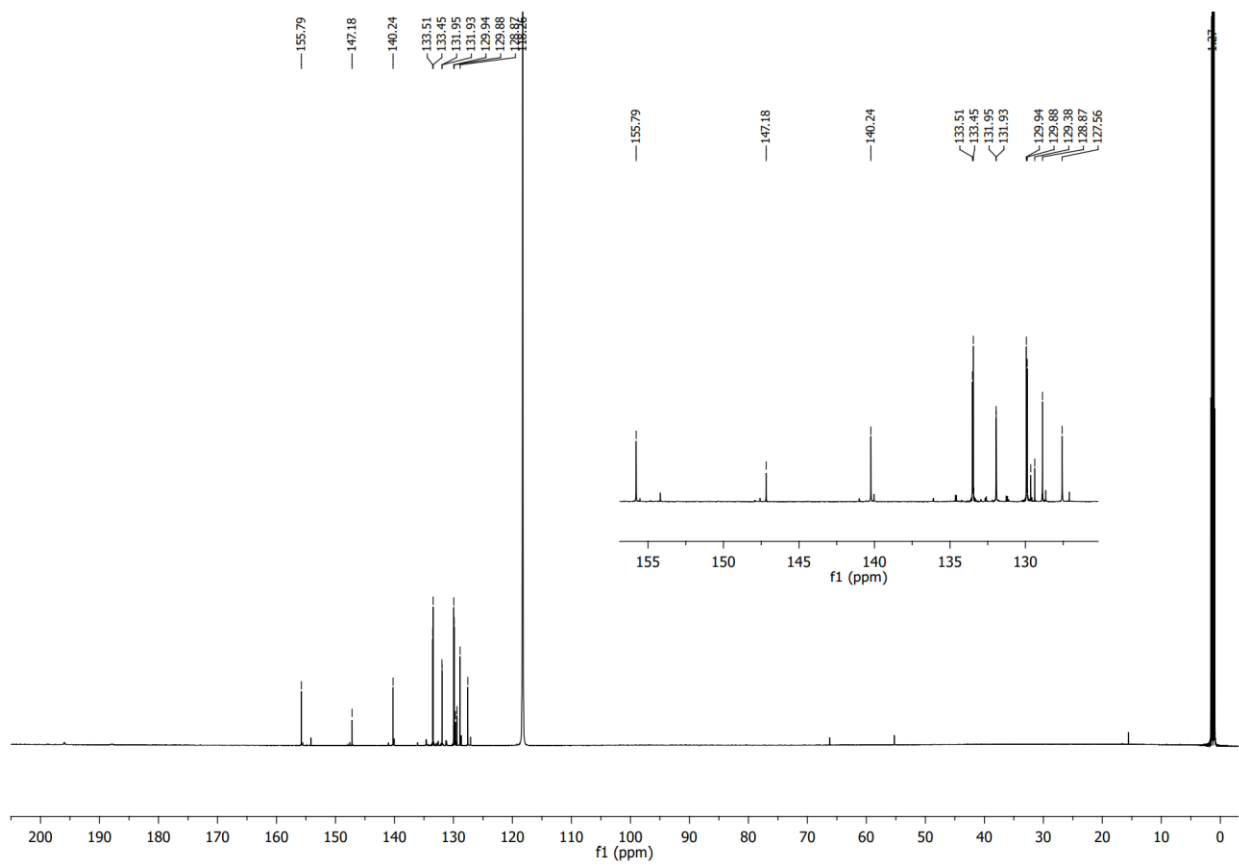


Figure S11. 176 MHz ^{13}C NMR of fac-[Re(phen)(CO)₃(PPh₃)](PF₆) (**Mod1**) in CD₃CN at 300K .



Figure S12. HR-ESIMS of fac-[Re(phen)(CO)₃(PPh₃)](PF₆) (**Mod1**).

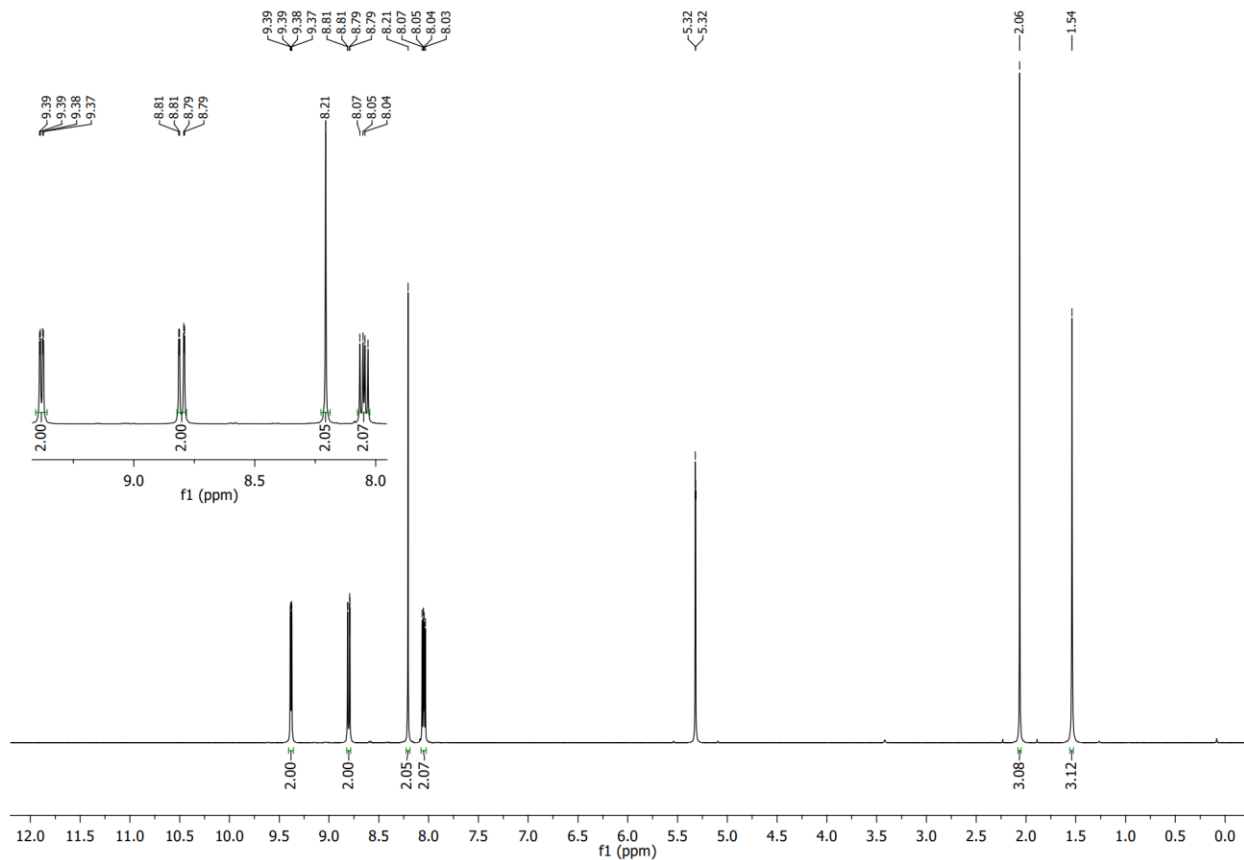


Figure S13. 700 MHz ^1H NMR of fac-[Re(phen)(CO)₃(CH₃CN)](PF₆) (**Mod2**) in CD₂Cl₂ at 300K.

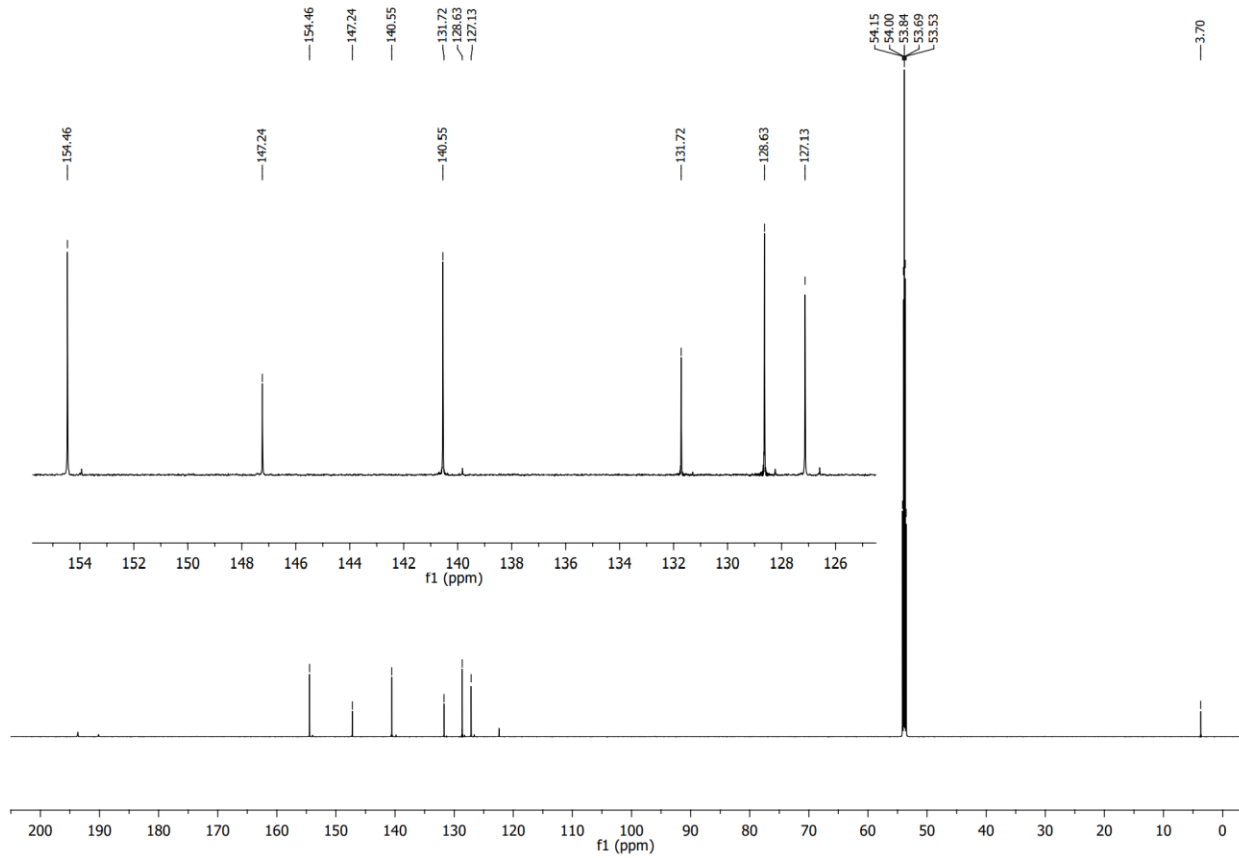


Figure S14. 176 MHz ^{13}C NMR of fac-[Re(phen)(CO)₃(CH₃CN)][PF₆] (**Mod2**) in CD₂Cl₂ at 300K.



Figure S15. HR-ESIMS of fac-[Re(phen)(CO)₃(CH₃CN)](PF₆) (**Mod2**).

Additional Computational Data

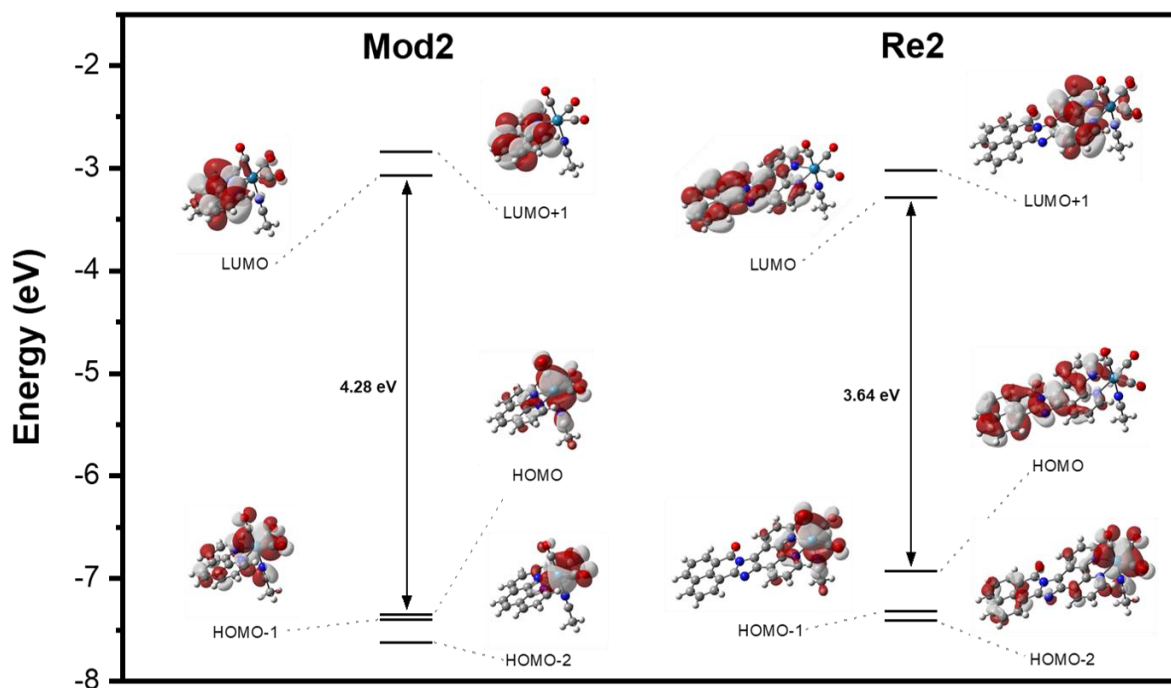


Figure S16. Frontier molecular orbital diagrams of the model Re(I)-CDI complex **Mod2** and corresponding NBI-phen complex **Re2**, where L = CH_3CN .

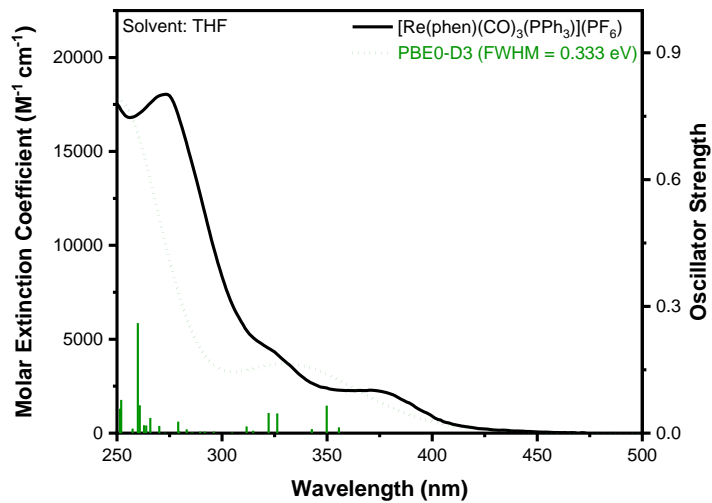


Figure S17. Experimental electronic absorption spectra overlay of **Mod1** with calculated singlet excited states.

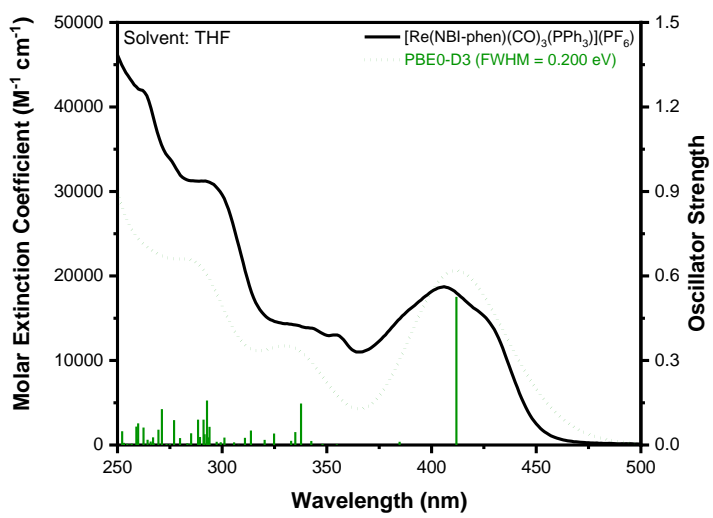


Figure S18. Experimental electronic absorption spectra overlay of **Re1** with calculated singlet excited states.

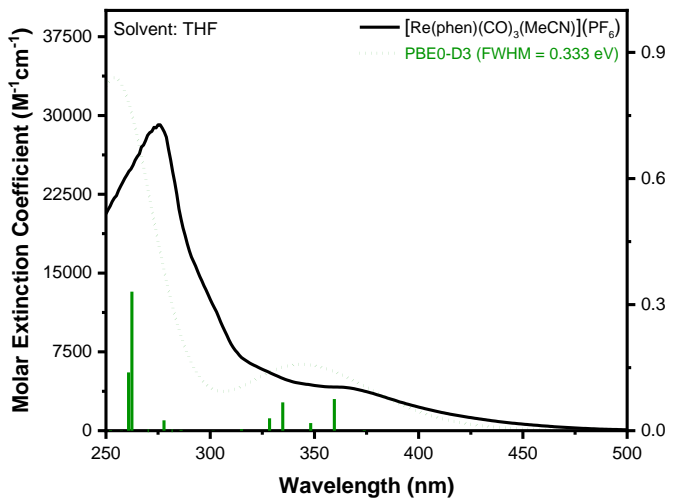


Figure S19. Experimental electronic absorption spectra overlay of **Mod2** with calculated singlet excited states.

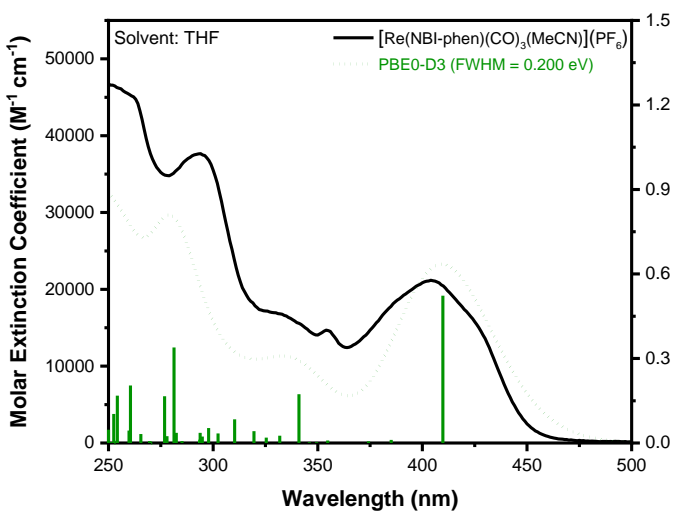


Figure S20. Experimental electronic absorption spectra overlay of **Re2** with calculated singlet excited states.

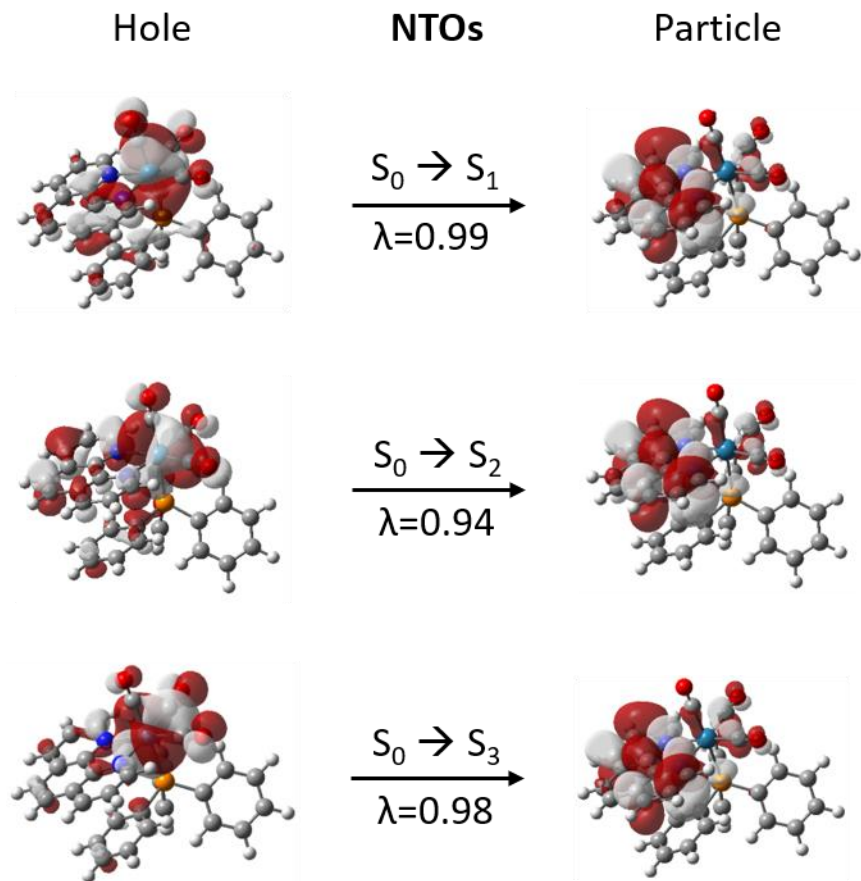


Figure S21. Natural transition orbitals for the three lowest transitions of **Mod1** predicted via TD-DFT at the PBE0-D3/Def2-SVP level of theory; λ is the fraction of the hole–particle contribution to the excitation.

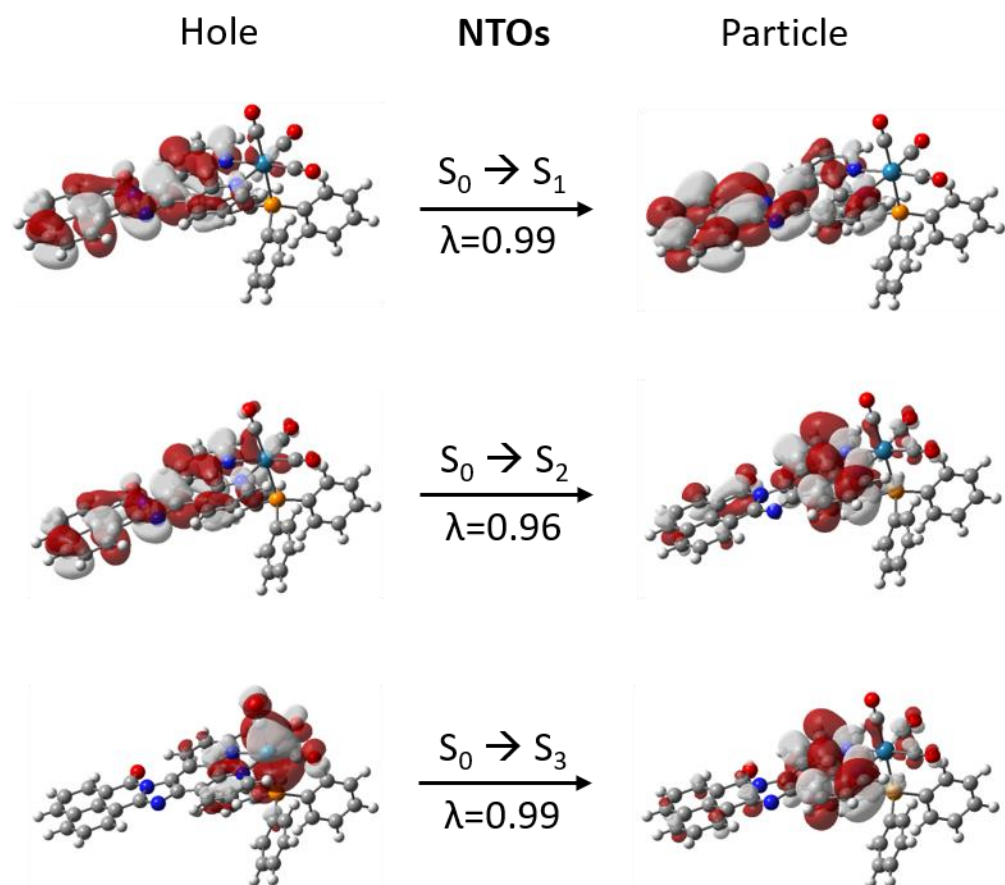


Figure S22. Natural transition orbitals for the three lowest transitions of **Re1** predicted via TD-DFT at the PBE0-D3/Def2-SVP level of theory; λ is the fraction of the hole–particle contribution to the excitation.

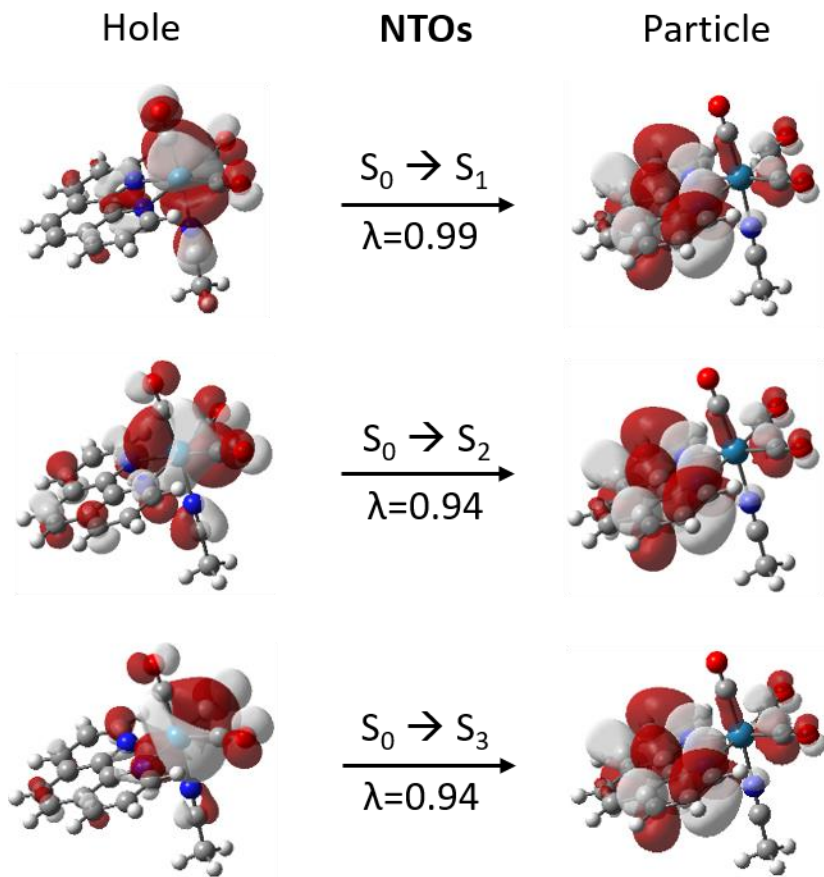


Figure S23. Natural transition orbitals for the three lowest transitions of **Mod2** predicted via TD-DFT at the PBE0-D3/Def2-SVP level of theory; λ is the fraction of the hole–particle contribution to the excitation.

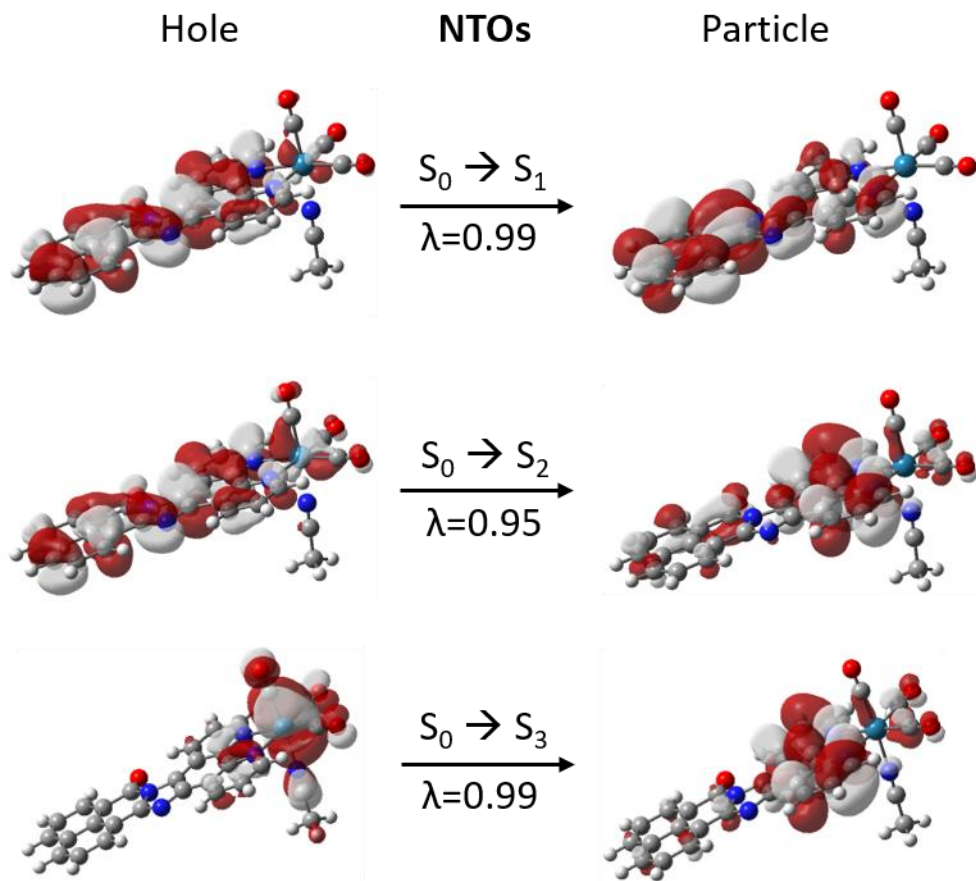
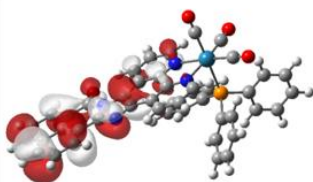


Figure S24. Natural transition orbitals for the three lowest transitions of **Re2** predicted via TD-DFT at the PBE0-D3/Def2-SVP level of theory PCM: THF; λ is the fraction of the hole–particle contribution to the excitation.

Table S1. Selected electronic excitation energies (nm) and corresponding oscillator strengths (f) of the low-lying singlet excited states of complexes **Mod1-2** and **Re1-2**.

molecule	$S_0 \rightarrow S_1$ /nm (f)	$S_0 \rightarrow S_2$ /nm (f)	$S_0 \rightarrow S_3$ /nm (f)
Mod1	355.6 (0.0136)	349.8 (0.0650)	342.7 (0.0095)
Re1	411.9 (0.5259)	384.7 (0.0114)	354.8 (0.0026)
Mod2	373.9 (0.0016)	359.6 (0.0754)	348.2 (0.0179)
Re2	409.7 (0.5234)	385.1 (0.0107)	374.3 (0.0056)

Singly Occupied Ligand Natural Orbitals



Occ. # = 1



Occ. # = 1

Doubly Occupied d π Natural Orbitals



Occ. # = 2



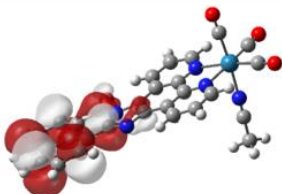
Occ. # = 2



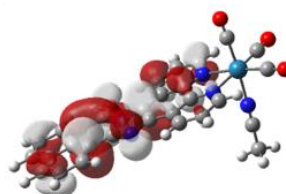
Occ. # = 2

Figure S25. Natural orbitals of **Re1**. PBE0-D3/Def2-SVP level of theory PCM: THF.

Singly Occupied Ligand Natural Orbitals

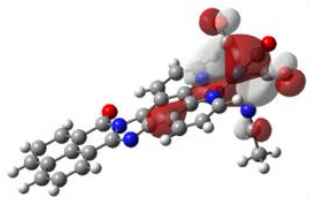


Occ. # = 1

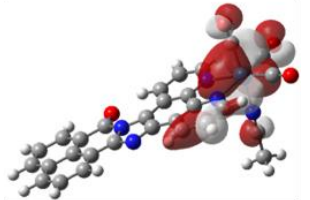


Occ. # = 1

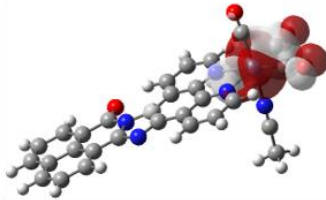
Doubly Occupied d π Natural Orbitals



Occ. # = 2



Occ. # = 2



Occ. # = 2

Figure S26. Natural orbitals of **Re2**. PBE0-D3/Def2-SVP level of theory PCM: THF.

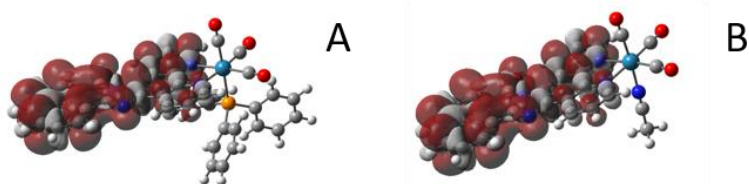


Figure S27. Triplet spin densities of (A) **Re1** and (B) **Re2**. PBE0-D3/Def2-SVP level of theory PCM: THF.

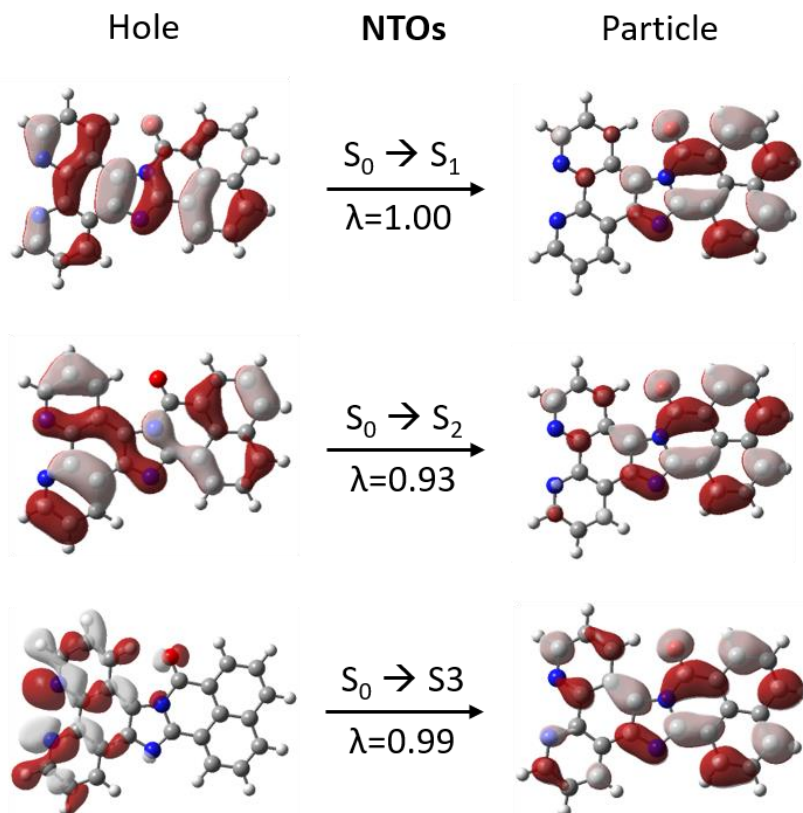


Figure S28. Natural transition orbitals for the three lowest transitions of **NBI-phen** predicted via TD-DFT at the PBE0-D3/Def2-SVP level of theory PCM: THF; λ is the fraction of the hole–particle contribution to the excitation.

Table S2. Optimized singlet geometries of **Re1-2** and **Mod1-2**:

Optimized geometry of **Re1**:

Re	-2.45645997	-0.20208138	-1.53399293
C	-2.17212009	-0.46227691	-3.45175425
O	-2.02594601	-0.61172225	-4.57897127
C	-3.93899404	-1.43045975	-1.59580505
O	-4.79768683	-2.20024091	-1.63383305
C	-3.63880734	1.27818846	-1.90622157
O	-4.30214052	2.19331246	-2.12960988
N	-0.60297767	0.97665377	-1.40605167

C	0.52659900	0.29161461	-1.09110719
C	-0.54554445	2.28954390	-1.60245351
C	1.79209057	0.93474938	-0.94906498
C	0.36289173	-1.12635400	-0.90257692
C	0.65488988	2.99378068	-1.51082495
H	-1.47915616	2.79905807	-1.84268125
C	1.81712197	2.32570552	-1.18763138
C	2.89660427	0.09019857	-0.57106029
C	1.46360135	-1.93362932	-0.56860550
N	-0.87904087	-1.65206793	-1.06902122
H	0.66003834	4.07000127	-1.68527036
H	2.76008352	2.85670189	-1.09108957
C	2.72648259	-1.28624483	-0.40466804
N	4.26227523	0.28941349	-0.31140836
C	1.27012861	-3.31776483	-0.41515648
C	-1.04358338	-2.96529029	-0.94075586
N	3.88624385	-1.91528238	-0.07794875
C	4.78980223	-0.97421542	-0.02709029
C	5.03736308	1.47350941	-0.24704255
H	2.11964275	-3.95045353	-0.15250228
C	0.00591234	-3.83317905	-0.61230653
H	-2.04841600	-3.35336234	-1.10939516
C	6.19092655	-1.15323595	0.27903931
C	6.46990467	1.28078362	0.04775129
O	4.54527267	2.56491221	-0.41796182
H	-0.19719912	-4.90020856	-0.51580187
C	7.01509287	-0.00255013	0.30337721
C	6.72862842	-2.40497673	0.53882432
C	7.28964410	2.39976062	0.07930209
C	8.40216566	-0.13710497	0.59343579
C	8.09920988	-2.53901691	0.82604534
H	6.07493402	-3.27885793	0.51480542
C	8.66106536	2.27162838	0.36031969
H	6.84939461	3.37886395	-0.11896604
C	9.20724333	1.02928899	0.61318381
C	8.92179327	-1.43096220	0.85277169
H	8.51034970	-3.53010540	1.02769740
H	9.29246658	3.16193488	0.37840379
H	10.27301753	0.92993101	0.83355744
H	9.98624542	-1.53723759	1.07541190
P	-2.74022222	0.19854449	0.94930748
C	-2.33306832	-1.22409856	2.03027645
C	-2.84972260	-2.47184375	1.65426307
C	-1.62696289	-1.11221507	3.23458008
C	-2.63992262	-3.59411460	2.45143389
H	-3.44124633	-2.56627490	0.74135155
C	-1.41313852	-2.23969254	4.02729947
H	-1.24443008	-0.14608866	3.56874642

C	-1.91134849	-3.48162875	3.63575329
H	-3.04937398	-4.55942830	2.14513281
H	-0.85670399	-2.14159676	4.96232347
H	-1.74025965	-4.36199955	4.25962442
C	-1.68175522	1.59306370	1.47434237
C	-2.20430397	2.89372523	1.46068780
C	-0.31609548	1.40704879	1.73461810
C	-1.37894900	3.98513455	1.72767129
H	-3.26192577	3.05866613	1.24105508
C	0.50376317	2.50143850	2.00129985
H	0.11943371	0.40540072	1.72727724
C	-0.02589807	3.79178968	2.00263787
H	-1.79943843	4.99329481	1.71904972
H	1.56614710	2.34246867	2.20090839
H	0.61945624	4.64812578	2.21122908
C	-4.40971393	0.65360273	1.54780826
C	-4.56110394	1.04610720	2.88704922
C	-5.53600218	0.56939723	0.72512111
C	-5.82048507	1.36151573	3.38591357
H	-3.68927459	1.10804946	3.54374814
C	-6.79906906	0.88260460	1.23010631
H	-5.43929652	0.25420342	-0.31369723
C	-6.94230935	1.28077341	2.55689660
H	-5.92860857	1.66984871	4.42832134
H	-7.67252596	0.81374621	0.57792031
H	-7.93118298	1.52754981	2.95061261

Optimized geometry of **Re2**:

Re	-2.45645997	-0.20208138	-1.53399293
C	-2.17212009	-0.46227691	-3.45175425
O	-2.02594601	-0.61172225	-4.57897127
C	-3.93899404	-1.43045975	-1.59580505
O	-4.79768683	-2.20024091	-1.63383305
C	-3.63880734	1.27818846	-1.90622157
O	-4.30214052	2.19331246	-2.12960988
N	-0.60297767	0.97665377	-1.40605167
C	0.52659900	0.29161461	-1.09110719
C	-0.54554445	2.28954390	-1.60245351
C	1.79209057	0.93474938	-0.94906498
C	0.36289173	-1.12635400	-0.90257692
C	0.65488988	2.99378068	-1.51082495
H	-1.47915616	2.79905807	-1.84268125
C	1.81712197	2.32570552	-1.18763138
C	2.89660427	0.09019857	-0.57106029
C	1.46360135	-1.93362932	-0.56860550
N	-0.87904087	-1.65206793	-1.06902122
H	0.66003834	4.07000127	-1.68527036

H	2.76008352	2.85670189	-1.09108957
C	2.72648259	-1.28624483	-0.40466804
N	4.26227523	0.28941349	-0.31140836
C	1.27012861	-3.31776483	-0.41515648
C	-1.04358338	-2.96529029	-0.94075586
N	3.88624385	-1.91528238	-0.07794875
C	4.78980223	-0.97421542	-0.02709029
C	5.03736308	1.47350941	-0.24704255
H	2.11964275	-3.95045353	-0.15250228
C	0.00591234	-3.83317905	-0.61230653
H	-2.04841600	-3.35336234	-1.10939516
C	6.19092655	-1.15323595	0.27903931
C	6.46990467	1.28078362	0.04775129
O	4.54527267	2.56491221	-0.41796182
H	-0.19719912	-4.90020856	-0.51580187
C	7.01509287	-0.00255013	0.30337721
C	6.72862842	-2.40497673	0.53882432
C	7.28964410	2.39976062	0.07930209
C	8.40216566	-0.13710497	0.59343579
C	8.09920988	-2.53901691	0.82604534
H	6.07493402	-3.27885793	0.51480542
C	8.66106536	2.27162838	0.36031969
H	6.84939461	3.37886395	-0.11896604
C	9.20724333	1.02928899	0.61318381
C	8.92179327	-1.43096220	0.85277169
H	8.51034970	-3.53010540	1.02769740
H	9.29246658	3.16193488	0.37840379
H	10.27301753	0.92993101	0.83355744
H	9.98624542	-1.53723759	1.07541190
P	-2.74022222	0.19854449	0.94930748
C	-2.33306832	-1.22409856	2.03027645
C	-2.84972260	-2.47184375	1.65426307
C	-1.62696289	-1.11221507	3.23458008
C	-2.63992262	-3.59411460	2.45143389
H	-3.44124633	-2.56627490	0.74135155
C	-1.41313852	-2.23969254	4.02729947
H	-1.24443008	-0.14608866	3.56874642
C	-1.91134849	-3.48162875	3.63575329
H	-3.04937398	-4.55942830	2.14513281
H	-0.85670399	-2.14159676	4.96232347
H	-1.74025965	-4.36199955	4.25962442
C	-1.68175522	1.59306370	1.47434237
C	-2.20430397	2.89372523	1.46068780
C	-0.31609548	1.40704879	1.73461810
C	-1.37894900	3.98513455	1.72767129
H	-3.26192577	3.05866613	1.24105508
C	0.50376317	2.50143850	2.00129985
H	0.11943371	0.40540072	1.72727724

C	-0.02589807	3.79178968	2.00263787
H	-1.79943843	4.99329481	1.71904972
H	1.56614710	2.34246867	2.20090839
H	0.61945624	4.64812578	2.21122908
C	-4.40971393	0.65360273	1.54780826
C	-4.56110394	1.04610720	2.88704922
C	-5.53600218	0.56939723	0.72512111
C	-5.82048507	1.36151573	3.38591357
H	-3.68927459	1.10804946	3.54374814
C	-6.79906906	0.88260460	1.23010631
H	-5.43929652	0.25420342	-0.31369723
C	-6.94230935	1.28077341	2.55689660
H	-5.92860857	1.66984871	4.42832134
H	-7.67252596	0.81374621	0.57792031
H	-7.93118298	1.52754981	2.95061261

Optimized geometry of **Mod1**:

Re	0.04581263	-1.55954082	-0.47377045
C	1.09334822	-3.11516865	-1.01408312
O	1.69763302	-4.03355411	-1.34035010
C	-0.95361345	-2.66494580	0.74973389
O	-1.50840994	-3.32126959	1.51632910
C	-1.22841805	-1.98581129	-1.85544675
O	-1.97299652	-2.27136083	-2.68914463
N	1.37448755	-0.17633249	-1.56600978
C	2.38888315	0.33864077	-0.82176428
C	1.25735145	0.20351250	-2.83461137
C	3.30364383	1.28416566	-1.33491391
C	2.52657806	-0.12562921	0.52541059
C	2.11600400	1.14040509	-3.42439829
H	0.45510533	-0.25451620	-3.41372324
C	3.13529725	1.69078399	-2.67431979
C	4.34799182	1.77646180	-0.48645306
C	3.58666172	0.34782574	1.32880566
N	1.62037804	-1.03091938	0.97169863
H	1.96331694	1.41745922	-4.46799741
H	3.81754616	2.42579471	-3.10702786
C	4.48607902	1.32419721	0.79111247
C	3.69981895	-0.18046643	2.63101290
C	1.75348842	-1.51817733	2.20141614
H	4.50657954	0.15858376	3.28453733
C	2.78837000	-1.12384120	3.05899421
H	1.00941303	-2.24715044	2.52663375
H	2.84659551	-1.55952643	4.05693863
H	5.03940303	2.51828408	-0.89134312
H	5.29028151	1.69700493	1.42851203
P	-1.19242632	0.55017993	0.23187240

C	-2.71499978	0.28583025	1.21237808
C	-3.56611048	-0.75858711	0.82891869
C	-3.10537448	1.14911062	2.24450971
C	-4.78380578	-0.94750778	1.47871497
H	-3.28300948	-1.42431920	0.01017999
C	-4.32133757	0.95153239	2.89650778
H	-2.46346349	1.97898141	2.54751867
C	-5.16039209	-0.09635296	2.51746891
H	-5.43881413	-1.76604745	1.17201717
H	-4.61478031	1.62515485	3.70499488
H	-6.11241835	-0.24819322	3.03150577
C	-1.78899955	1.69087523	-1.07493006
C	-2.20140372	2.98635680	-0.72469312
C	-1.91741155	1.27130305	-2.40152786
C	-2.70823663	3.84725307	-1.69317745
H	-2.12461050	3.32915279	0.31011424
C	-2.42769599	2.13513475	-3.37132666
H	-1.63891718	0.25863860	-2.68657138
C	-2.81841674	3.42484047	-3.02000371
H	-3.02293839	4.85418310	-1.40956168
H	-2.52150074	1.79184818	-4.40401886
H	-3.21688201	4.10273678	-3.77852251
C	-0.09372998	1.59180433	1.25423528
C	0.11303745	1.26999947	2.60334949
C	0.66404889	2.61714621	0.66997793
C	1.04083589	1.98224466	3.36003396
H	-0.45351839	0.45882701	3.06797573
C	1.59368595	3.32397490	1.43110284
H	0.52985669	2.87090784	-0.38404640
C	1.78071687	3.01136603	2.77676418
H	1.18932980	1.72657771	4.41156040
H	2.17585341	4.12213260	0.96550554
H	2.50877742	3.56692383	3.37222990

Optimized geometry of **Mod2**:

Re	1.15018878	0.00103779	-0.18968860
C	1.32370252	0.00576094	-2.11543094
O	1.41754390	0.00849101	-3.26103014
C	2.51830923	1.35954495	-0.07145149
O	3.30984207	2.19207453	0.00072312
C	2.51851938	-1.35785278	-0.07811421
O	3.31014769	-2.19063001	-0.00999425
N	0.80997841	-0.00505652	1.92496492
C	0.58809199	-0.01052184	3.05767531
C	0.32174367	-0.01902086	4.47630931
H	1.09666887	-0.60332559	4.99303344
H	0.32793567	1.01105259	4.86035494

H	-0.66167467	-0.47201487	4.66623848
N	-0.59239501	-1.34529677	-0.22584539
C	-1.79514433	-0.71557391	-0.20395117
C	-0.56173132	-2.67311838	-0.23745606
C	-3.01979681	-1.41813482	-0.19137527
C	-1.79521183	0.71719115	-0.20043293
C	-1.72792309	-3.45181017	-0.22708044
H	0.42306777	-3.14350485	-0.25651509
C	-2.95825066	-2.82774402	-0.20294537
C	-4.24851623	-0.68066123	-0.17107125
C	-3.01993301	1.41956357	-0.18445936
N	-0.59253426	1.34713076	-0.21924247
H	-1.64232961	-4.53898350	-0.23895387
H	-3.88214721	-3.41033341	-0.19468880
C	-4.24857921	0.68187828	-0.16774380
C	-2.95853085	2.82921650	-0.18916957
C	-0.56199765	2.67499386	-0.22436048
H	-3.88247710	3.41168083	-0.17819427
C	-1.72825948	3.45350968	-0.21019585
H	0.42276261	3.14554415	-0.24108727
H	-1.64277355	4.54073846	-0.21676301
H	-5.18881830	-1.23590853	-0.16101052
H	-5.18894006	1.23696829	-0.15497658

Additional Spectroscopic Data

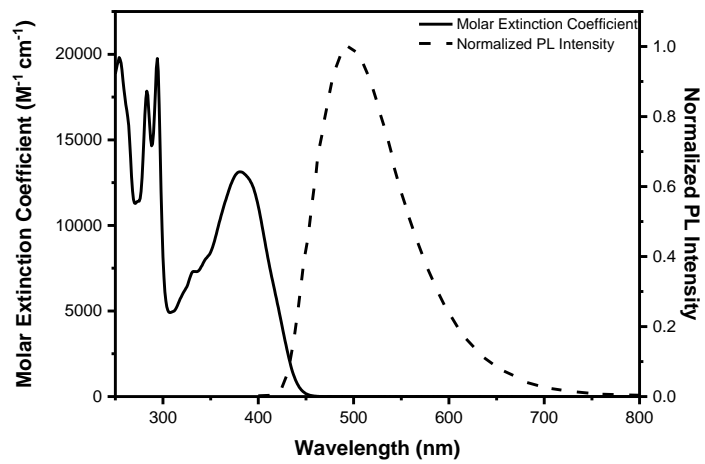


Figure S29. Electronic absorption spectra and PL of **NBI** in THF.

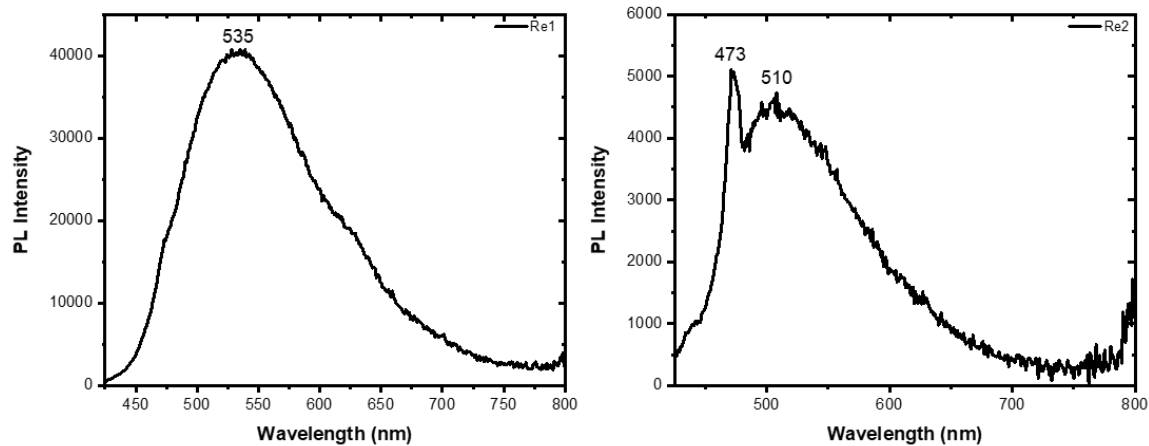


Figure S30. Aerated PL of **Re1** (left) and **Re2** (right). Feature at 473 nm is Raman band of THF excited at 415 nm.

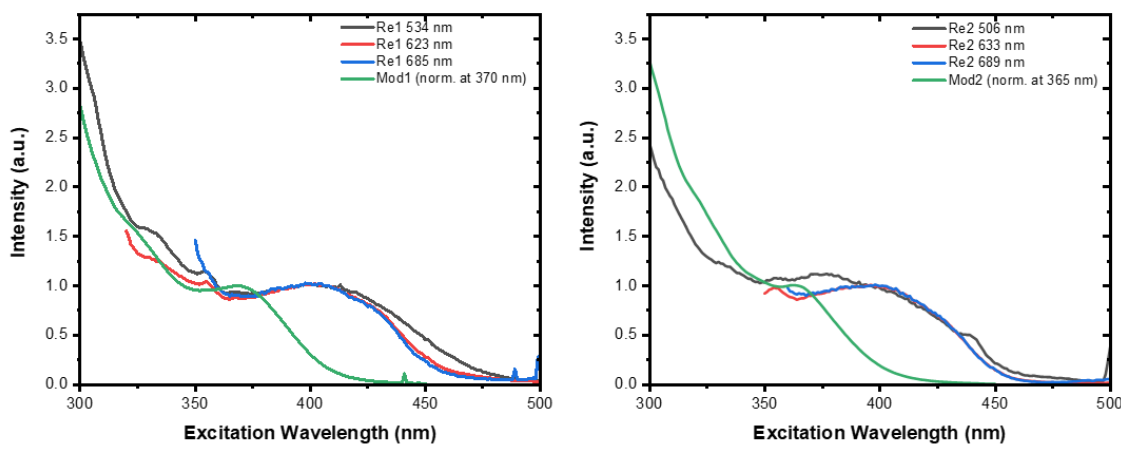


Figure S31. Excitation scans of **Re1**, **Mod1** (left) and **Re2**, **Mod2** (right). Monitored PL peak is denoted in the legend.

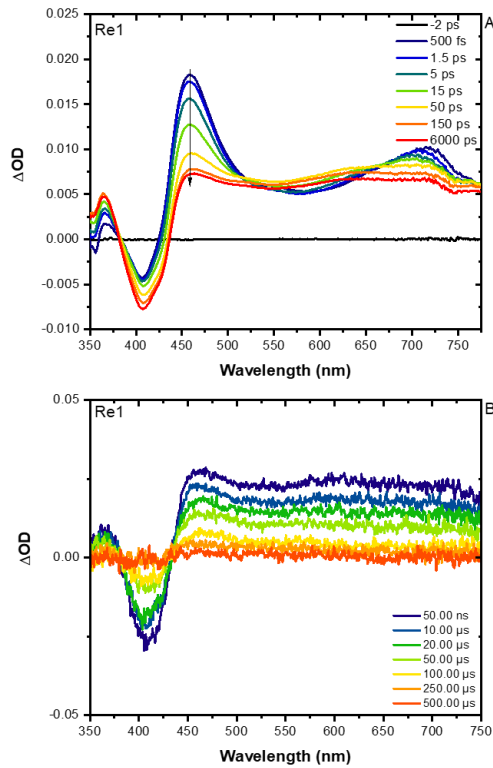


Figure S32. UFTA of (A) **Re1** in THF following 400 nm pulsed laser excitation (105 fs fwhm, 0.3 mJ/pulse) and (B) nsTA of **Re1** in deaerated THF following 415 nm excitation (1.8 mJ/pulse).

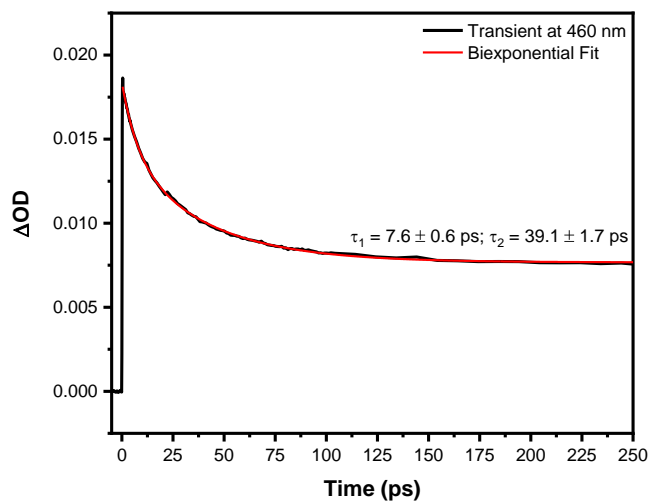


Figure S33. Ultrafast transient absorption kinetic data of **Re1** in THF following 400 nm pulsed excitation. Single wavelength kinetic analysis at 460 nm.

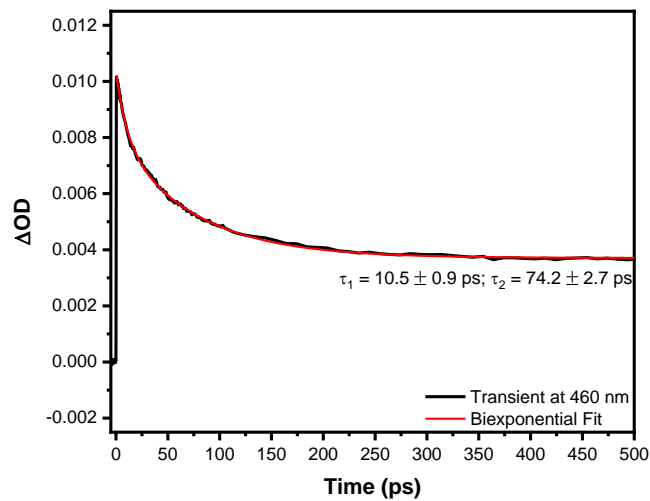


Figure S34. Ultrafast transient absorption kinetic data of **Re2** in THF following 400 nm pulsed excitation. Single wavelength kinetic analysis at 460 nm.

Table S3. Data table of **Re1** rate constants and beta values after fitting using the TTA fitting equation from Deng et. al.³ Experiments were carried out in deaerated THF ($\lambda_{\text{ex}} = 415 \text{ nm}$).

Power (mJ/pulse)	$k_T (\text{ns}^{-1})$	$k_T (\text{s}^{-1})$	β
2.0	1.34E-6	1.34E3	0.940
1.6	1.70E-6	1.70E3	0.909

1.2	1.95E-6	1.95E3	0.885
0.8	2.21E-6	2.21E3	0.834

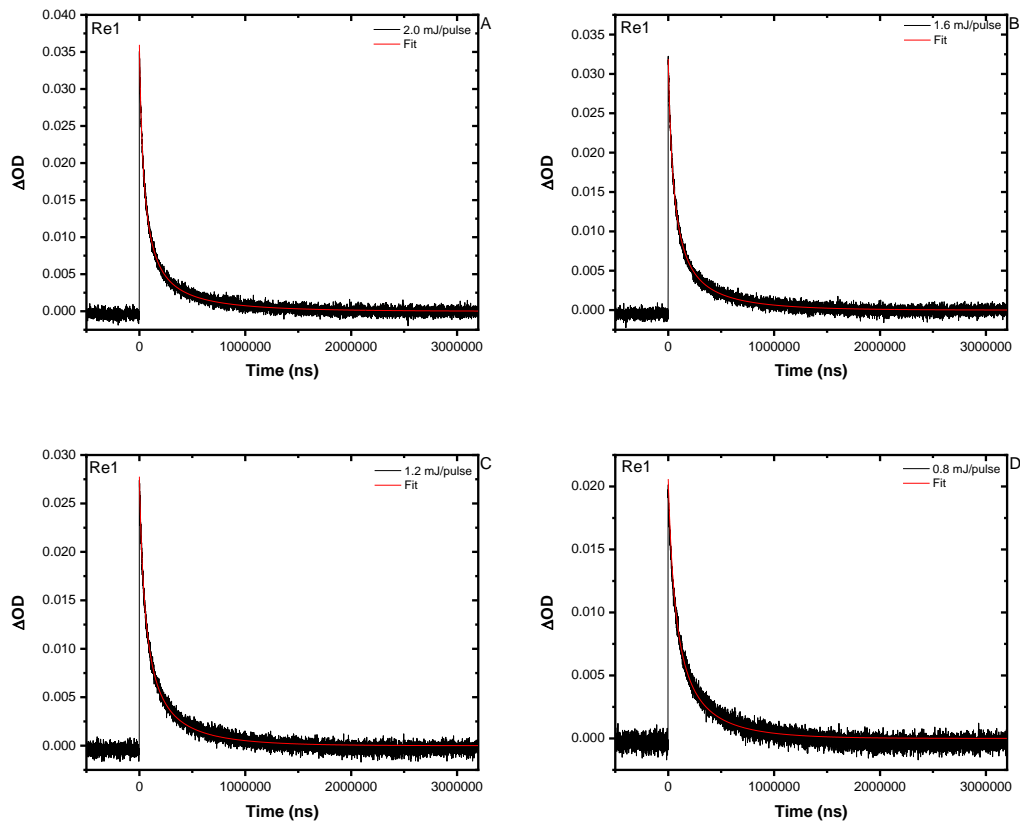


Figure S35. Kinetic traces and fits of **Re1** at 2.0 (A), 1.6 (B), 1.2 (C), and 0.8 (D) mJ/pulse in deaerated THF ($\lambda_{\text{ex}} = 415$ nm).

Table S4. Data table of **Re2** rate constants and beta values after fitting using the TTA fitting equation from Deng et. al.³ Experiments were carried out in deaerated THF ($\lambda_{\text{ex}} = 415$ nm).

Power (mJ/pulse)	$k_T (\text{ns}^{-1})$	$k_T (\text{s}^{-1})$	β
2.0	1.75E-6	1.75E3	0.956
1.7	2.18E-6	2.18E3	0.942
1.4	2.70E-6	2.70E3	0.923
1.0	3.14E-6	3.14E3	0.906

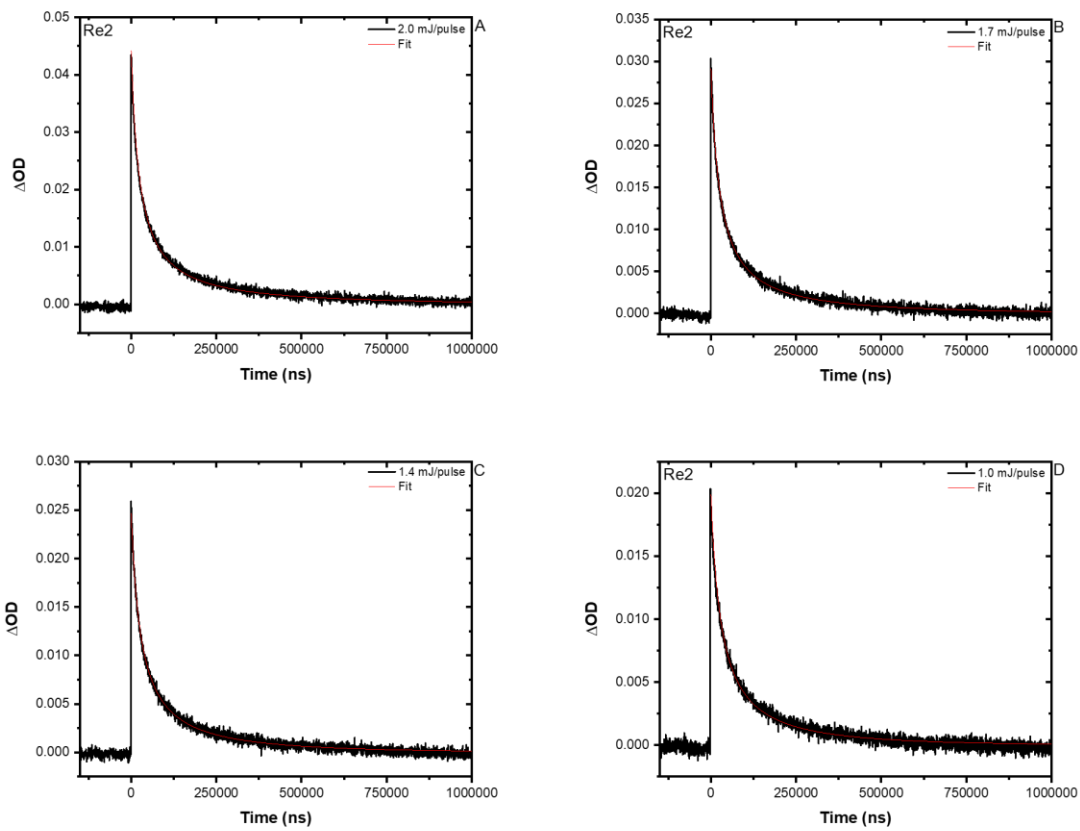


Figure S36. Kinetic traces and fits of **Re2** at 2.0 (A), 1.7 (B), 1.4 (C), and 1.0 (D) mJ/pulse in deaerated THF ($\lambda_{\text{ex}} = 415 \text{ nm}$).

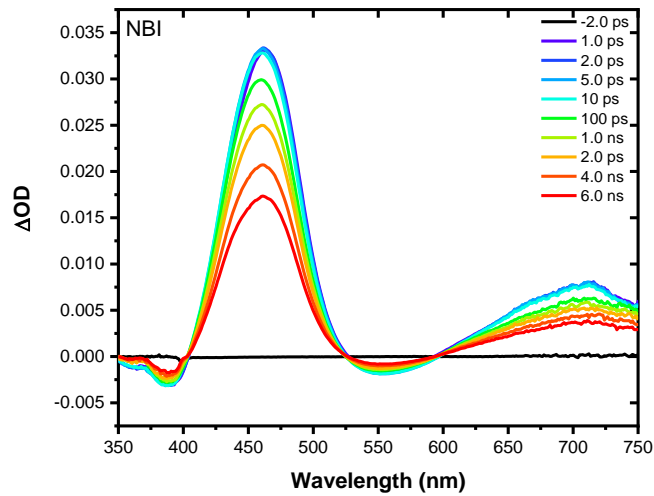


Figure S37. UFTA of **NBI** in THF following 400 nm pulsed laser excitation (105 fs fwhm, 0.5 mJ/pulse).

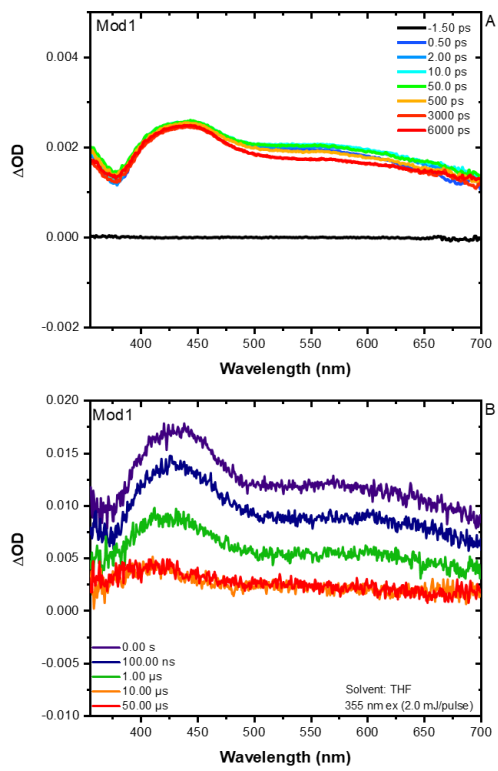


Figure S38. Nanosecond transient absorption spectra of (A) UFTA of **Mod1** following 350 nm excitation (105 fs fwhm, 50 μ J/pulse) in THF and (B) nsTA of **Mod1** following 355 nm excitation (1.8 mJ/pulse) in deaerated THF.

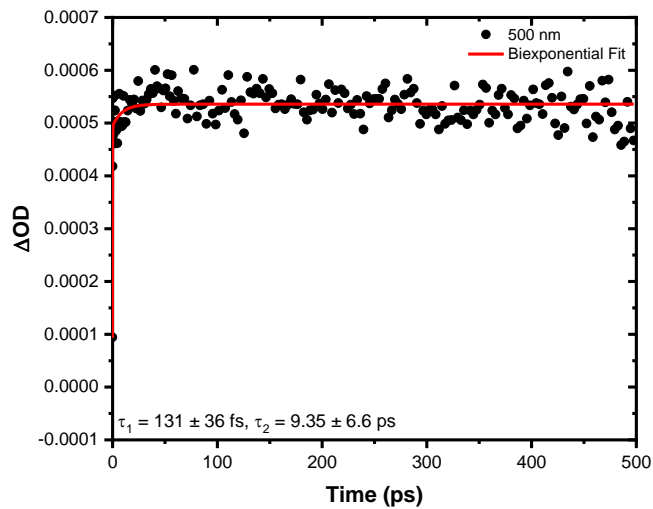


Figure S39. Ultrafast transient absorption kinetic data of **Mod1** following 350 nm excitation (105 fs fwhm, 50 μ J/pulse) in THF. Single wavelength kinetic analysis at 500 nm.

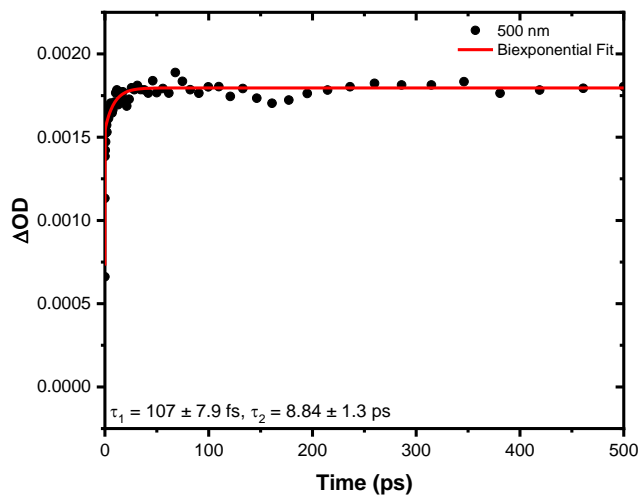


Figure S40. Ultrafast transient absorption kinetic data of **Mod2** following 350 nm excitation (105 fs fwhm, 50 $\mu\text{J}/\text{pulse}$) in THF. Single wavelength kinetic analysis at 500 nm.

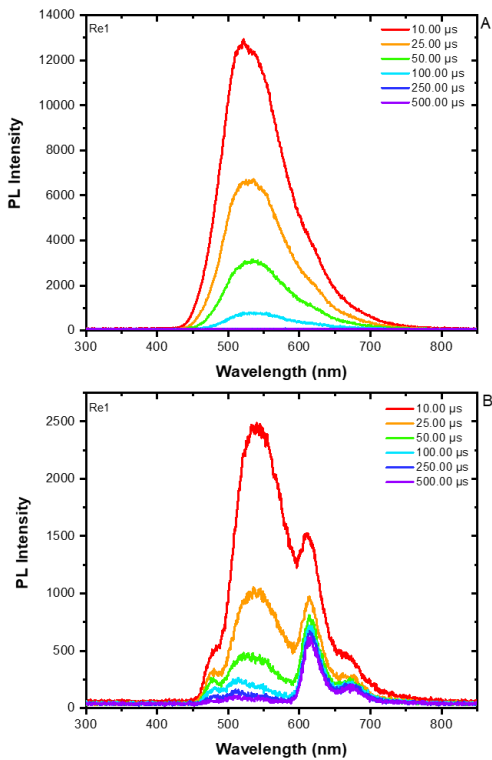


Figure S41. Time-resolved photoluminescence data of **Re1** at (A) room temperature in deaerated THF and (B) 77 K in 2-MeTHF following 415 nm excitation (1.8 mJ/pulse).

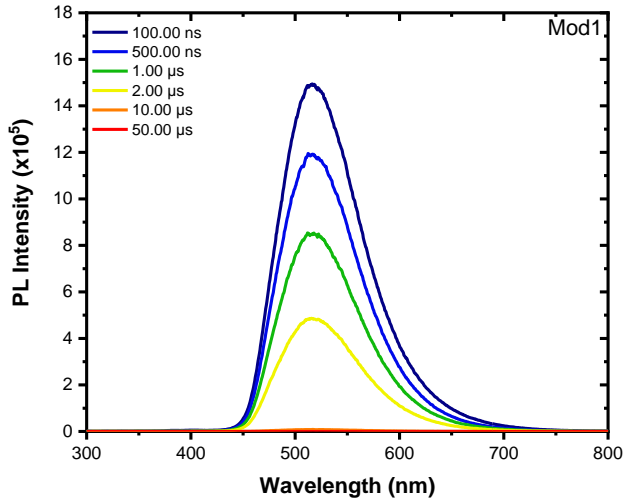


Figure S42. Time-resolved photoluminescence spectra of **Mod1** after excitation using a Continuum Minilite with 355 nm pulsed excitation (2.0 mJ/pulse, 5 ns fwhm).

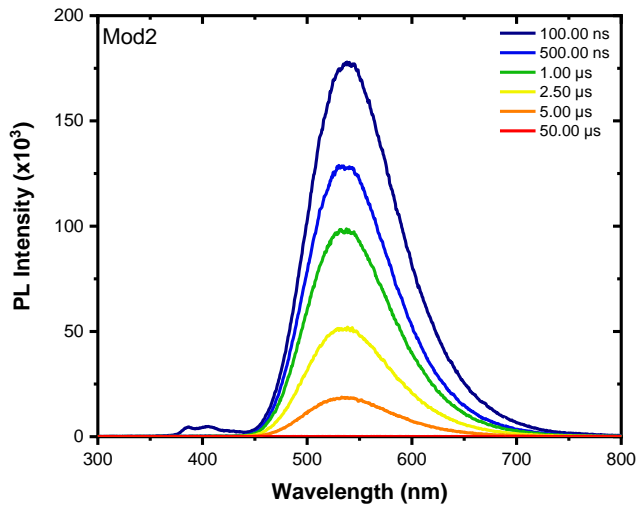


Figure S43. Time-resolved photoluminescence spectra of **Mod2** after excitation using a Continuum Minilite with 355 nm pulsed excitation (2.0 mJ/pulse, 5 ns fwhm).

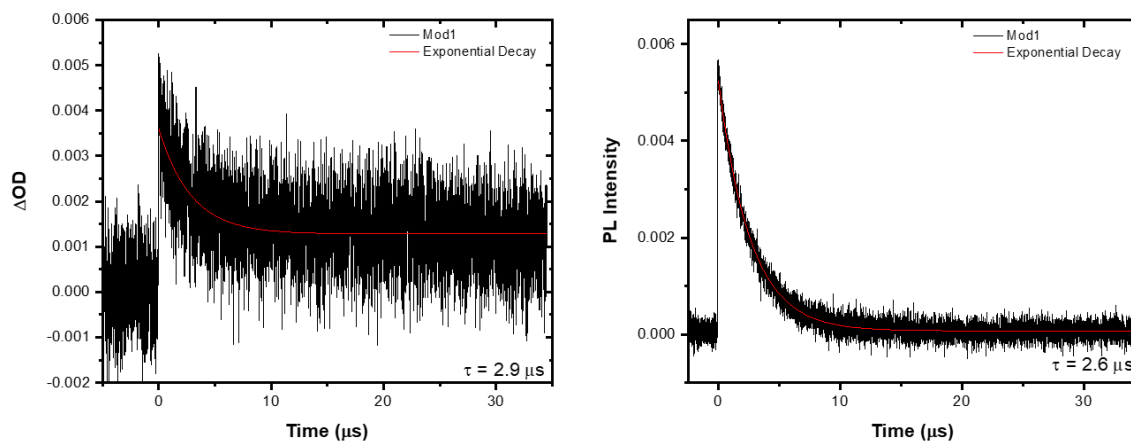


Figure S44. nsTA kinetics (left) and PL kinetics (right) of **Mod1** in THF after excitation using a Continuum Minilite with 355 nm pulsed excitation (2.0 mJ/pulse, 5 ns fwhm). Intense noise on nsTA kinetics due to a ND filter being placed in front of Xe arc lamp to reduce amount of decomposition of sample.

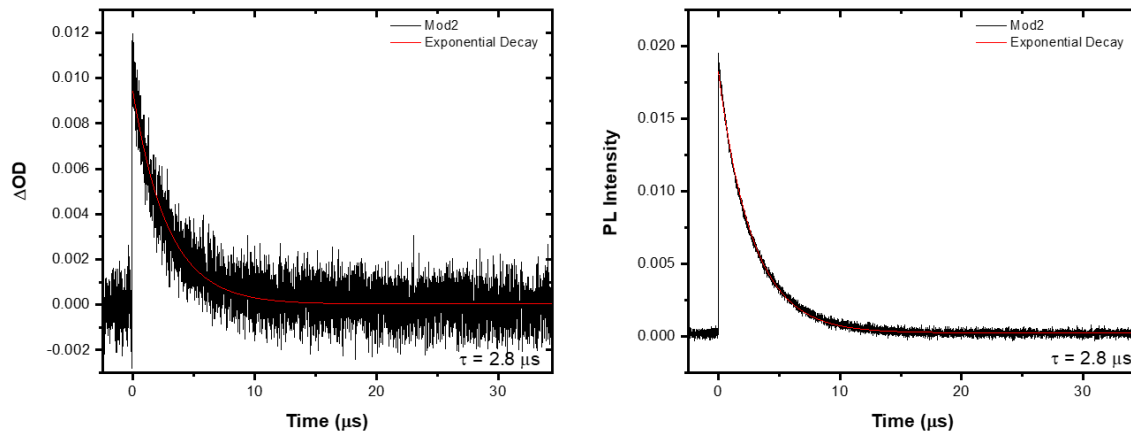


Figure S45. nsTA kinetics (left) and PL kinetics (right) of **Mod2** in THF after excitation using a Continuum Minilite with 355 nm pulsed excitation (2.0 mJ/pulse, 5 ns fwhm).

References:

1. Y. Yang, J. Brückmann, W. Frey, S. Rau, M. Karnahl and S. Tschierlei, *Chem. Eur. J.*, 2020, **26**, 17027-17034.
2. J. E. Yarnell, K. A. Wells, J. R. Palmer, J. M. Breaux and F. N. Castellano, *J. Phys. Chem. B*, 2019, **123**, 7611-7627.
3. F. Deng, J. Blumhoff and F. N. Castellano, *J. Phys. Chem. A*, 2013, **117**, 4412-4419.